Aalto University
School of Science

Master’s Programme in Mathematics and Operations Research

Optimising a Renewable Virtual Power Plant in Day-ahead, Intraday and Balancing Markets

Tuomas Mäkelä

Master’s Thesis
2024

Aalto University
School of Science

Author Tuomas Mäkelä

Title Optimising a Renewable Virtual Power Plant in Day-ahead, Intraday and Balancing Markets

Degree programme Mathematics and Operations Research

Major Systems and Operations Research

Supervisor Associate Prof. Fabricio Oliveira

Advisor Jaakko Kiviluoma (MSc.)

Collaborative partner St1 Nordic Oy

Date December 20, 2024 **Number of pages** 71 **Language** English

Abstract

The Nordic electricity market has significantly changed during the past years. The rapid increase of renewable generation, through wind and solar power, the opening of the largest nuclear reactor in Europe, and the phase-out of fossil fuels has coincided with historic levels of price volatility in Finland. Simultaneously, inflation has caused investment costs to rise sharply while interest rates have seen their highest peak in over a decade. Amidst these changes, renewable generation and consumption have faced challenges in sustaining the rapid buildout seen during the past few years, which is essential in reducing greenhouse gas emissions and transitioning to a low-carbon society.

The objective of this thesis is to propose a stochastic dual dynamic programming tool to support the operation of a renewable power market portfolio, consisting of variable renewable generation and a dynamically operated electrolyser. The markets considered are the day-ahead market, the intraday market and the manual Frequency Restoration Reserve (mFRR) balancing energy market. The agent faces uncertainties regarding both their own renewable generation and the market price in different stages. Despite multi-market optimisation being a widely documented problem in the literature, this thesis is one of the first contributions to optimise decision-making at discrete time points in a Finnish context. Furthermore, research on the optimisation of renewable fuels of non-biological origin (RFNBO hydrogen) remains limited, especially in a context concerning price uncertainty.

Experimental results indicate that the profit improvement was 4.18% for the optimal model when compared to a baseline strategy emulating the default operation of a market participant. The main driver of the profit improvement was the more strategic overbuying- or selling of energy, with the intention of covering the opened positions at a later market stage, resulting in the agent finding profitable opportunities more often and allocating generation more efficiently. The profit improvement is not directly applicable to an actual participant in the same markets as the agent of this thesis. Nevertheless, the results suggest that a bidding model such as the model presented in this thesis can significantly improve market profits for a renewable portfolio.

Keywords SDDP, renewable energy, electricity markets

Aalto-yliopisto
Perustieteiden
korkeakoulu

Tekijä Tuomas Mäkelä

Työn nimi Uusiutuvan sähköportfolion optimointi vuorokausi-, intraday- sekä reservimarkkinoilla

Koulutusohjelma Mathematics and Operations Research

Pääaine Systems and Operations Research

Työn valvoja Associate Prof. Fabricio Oliveira

Työn ohjaaja KTM Jaakko Kiviluoma

Yhteistyötaho St1 Nordic Oy

Päivämäärä 3. joulukuuta 2024 **Sivumäärä** 71 **Kieli** englanti

Tiivistelmä

Pohjoismainen sähkömarkkina on muuttunut merkittävästi viime vuosina. Uusiutuvan tuuli- ja aurinkotuotannon kasvaneen määrän, Euroopan suurimman ydinreaktorin käyttöönoton sekä fossiilisten tuotantomenetelmien sulkemisen myötä markkinavolatiliteetti on kasvanut ennätykselliselle tasolle. Samalla inflaatio ja kasvaneet korkokulut ovat lisänneet investointikustannuksia merkittävästi, mikä on hidastanut uusiutuvan tuotannon ja kulutuksen rakentamista. Tämä kehitys vaikeuttaa kasvihuonepäästöjen vähentämistä ja siirtymistä vähähiiliseen yhteiskuntaan.

Tämän diplomityön tarkoituksena on tarkastella uusiutuvan sähkömarkkinaportfolion optimointia stokastisen ohjelmoinnin avulla. Työssä luodaan työkalu tukeemaan uusiutuvan tuotantoportfolion markkinakaupankäyntiä. Tarkasteltu portfolio koostuu tuuli- ja aurinkovoimasta sekä dynaamisesta uusiutuvan vedyn tuotantolaitoksesta, ja se toimii kolmella eri sähkömarkkinalla: vuorokausi-, intraday- ja reservimarkkinoilla. Muodostettu malli käy kauppaa neljässä diskreetissä aikapisteessä. Vaikka sähkömarkkinaoptimointia on tutkittu laajasti, markkinatuoton sekä uusiutuvan vedyntuotannon kokonaistuotannon optimointi suomalaisen yrityksen näkökulmasta on jäänyt vähemmälle huomiolle.

Kokeelliset tulokset osoittavat, että kokonaistuotto vuoden 2024 ensimmäisellä puoliskolla käyttäen optimaalista strategiaa parani 4,18% verrattuna tyypillistä operointilogiikkaa edustavaan verrokkistrategiaan. Parannus johtui erityisesti strategisesta yli- tai alimyynnistä aiemmilla markkinavaiheilla, tavoitteena sulkea positio myöhemmillä markkinoilla paremmalla hinnalla. Lisäksi optimoitu malli allokoi omaa tuotantoa tehokkaammin kuin verrokkistrategia. Vaikka kokonaistuoton paraneminen ei ole täysin verrattavissa todellisuuteen, työ osoittaa kuitenkin markkinaoptimoinnin potentiaalin uusiutuvan markkinaportfolion kannattavuuden tavoittelussa.

Avainsanat SDDP, uusiutuva energia, sähkömarkkinat

Preface

Though this thesis may not yet mark the end of my studies, it represents a meaningful opportunity to reflect on the past years I have spent at Aalto University. When I first arrived, my intention was to gain a deeper understanding of the world around me. Looking back, while the journey turned out differently than I initially expected, I am grateful to see that I have indeed succeeded in my goal. Though my knowledge of physics may not have grown as much as anticipated, by studying operations research I have developed a richer understanding of the society we are shaped by. The learnings and skills acquired during my studies will, I hope, enable me at some point to contribute to improving the world around us, one step at a time.

I would like to express my sincere gratitude to Associate Professor Fabricio Oliveira for his invaluable guidance throughout the writing of this thesis. I would also like to thank Jaakko Kiviluoma and my colleagues at St1 for providing me the opportunity to not only write this thesis, but also explore the challenges and opportunities within the green transition. Their support has allowed me to engage with this fascinating thesis topic, while also offering me a valuable perspective into the Nordic energy environment — one I fully intend to build upon in the future.

Finally, I would like to express my endless gratitude to the many friends who have provided me with invaluable advice and countless priceless memories. These truly have been the best years of my life. Whether it was the long days spent studying in the library, the early mornings, the late nights at Rektorsgatan and elsewhere, or the countless hours spent sharing the most unforgettable adventures, I have not once forgotten that I am surrounded by the most incredible people, whom I am lucky to call my friends. To the Guild of Physics, Raati '22, FTMK '22, Äpy 2025, KF Uono Maita <3, and most importantly, my family and my wonderful partner Lotta — thank you. Your support and companionship have made this journey truly special.

Otaniemi, December 20, 2024

Tuomas J. M. Mäkelä

Contents

Symbols and abbreviations

Abbreviations

SDDP	stochastic dual dynamic programming
SDDiP	stochastic dual dynamic integer programming
VPP	virtual power plant
VRE	variable renewable energy
TSO	transmission system operator
RFNBO	renewable fuel of non-biological origin
LC	low-carbon
Non-RFNBO	low-carbon and fossil based
DA	day-ahead market
IDA1	intraday auction one
IDA2	intraday auction two
IDA3	intraday auction 3
mFRR	manual frequency restoration reserve
aFRR	automatic frequency restoration reserve
FCR-N	frequency containment reserves for normal operation
FCR-D	frequency containment reserves for disturbances
SDAC	Single Day-Ahead Coupling
CHP	combined heat and power
SMR	steam-methane reformation
SAF	synthetic air fuel
PEM	photon exchange membrane
SOEC	solid oxide electrolysis
D & D-1	on specific day and day before
EET	Eastern European time
EU	European Union
UK	United Kingdom
CWE	Central Western Europe
FI	Finland power price area
SE1 - SE4	Sweden power price areas
NO1 - NO5	Norway power price areas
MW	megawatt
GW	gigawatt
TW	terawatt
MWh	megawatt hour
CPU	Central Processing Unit

Symbols

Sets

$\mathbb{U}$	Set of control variables
$\mathbb{G}$	Generation scenarios for the agent's own generation
$\mathbb{S}$	Price forecast scenarios for the three final stages
$\mathbb{M}$	Scenarios for regulation state in mFRR market

Variables

u_b	Control variable representing buy trade volume
u_s	Control variable representing sell trade volume
Λ	Power balance state variable
$\mathcal{P}$	Total available power variable
Δ^+	Positive imbalance
Δ^-	Negative imbalance
G	Value of agent generation
M_+	Theoretical upper bound for positive imbalance
M_-	Theoretical upper bound for negative imbalance
δ	Auxiliary binary variable to enforce imbalance variable exclusivity
E	Electrolyser capacity
R	RFNBO generation
γ_z	Capacity of a single generation asset
ψ_{DA}	Random residual of day-ahead forecast
ρ	Forecasted intraday price
ε_{IDA_k}	Maximum obtainable market volume at k-th IDA auction
ε_{mFRR}	Maximum obtainable market volume at mFRR stage
r^+	Binary indicator variable for up-regulation hour
r^-	Binary indicator variable for down-regulation hour
$\mu_{Surplus}$	Penalisation variable for surplus of power

Parameters

$E_{maximum}$	maximum electrolyser capacity
α	RFNBO percentage of price area
mp_{RFNBO}	marginal non-electricity profit of RFNBO hydrogen
$mp_{N-RFNBO}$	marginal non-electricity profit of non-RFNBO hydrogen
c_1	constant penalisation parameter for negative imbalance
c_2	constant penalisation parameter for positive imbalance

1 Introduction

The European power market has encountered significant change during the past decade. Political efforts to decrease carbon emissions amid growing concerns over climate change have resulted in an explosive increase of variable renewable generation. Simultaneously, a subsequent phase-out of fossil-powered assets has occurred, partly as a result of more renewable generation. Additionally, the electrification of society has accelerated, with power demand forecasted to increase substantially in the coming years. All these factors have significantly altered the central dynamics of producing and consuming energy. Furthermore, geopolitical tensions such as the Russian offense on Ukraine have changed the characteristics of the European power market for good. Thus, instead of a relatively stable and predictable market price, price fluctuations are common and sometimes even extreme, reaching prices close to the minimum or maximum market level.

One such European country that has commonly exhibited extreme price fluctuations has been Finland. In 2023, the Finnish power market was one of the most volatile electricity markets in the world. On one hand, Finland had the largest cumulative amount of negative hours in Europe, totalling 467 hours. However, in January of 2024, the Finnish day-ahead market reached a new record high of 1896 €/MWh when a cold spell and subsequent increase in demand coincided with low wind generation and plant shutdowns. [1]

There are many underlying factors for the increase in volatility. The variable renewable (VRE) generation capacity has reached a high of nearly 7.4 GW for wind (as of June 2024), while solar capacity has risen to over 1 GW [2, 3]. This high penetration of VREs affects volatility in multiple ways. Since the opening of the third largest nuclear reactor in the world, Olkiluoto 3, in March of 2023, the amount of stable baseload power has increased significantly. Thus, even a relatively normal amount of wind and solar generation may cause the residual load, i.e., the demand subtracted by the total nuclear, hydro, wind and solar generation, to become negative, which subsequently depresses prices due to an oversupply of zero marginal cost power. In contrast, this decreases the number of operational hours for fossil-powered assets, which are further down the merit order compared to low-carbon alternatives. Thus, to recoup the value of lost generation, prices are increased during the remaining hours of generation. The result is a large increase in day-ahead market volatility. [4, 5]

Furthermore, the importance of different markets in addition to the day-ahead market has increased significantly. Increasing amounts of power are traded in intraday markets and TSO-operated ancillary markets, which are central in enabling the continuous balancing of supply and demand. Volatility spills over to these markets as well; forecasting errors can cause significant deviation from day-ahead commitments, resulting in price peaks potentially hundreds of euros higher than day-ahead prices. The effect of VREs is also evident in Fingrid's ancillary markets, which have reached a whole new level of importance during the past decade.

Though volatility is a key instrument in providing incentives for consumers and generators, extreme volatility remains problematic from a government, consumer and grid operator perspective. Negative prices may be an indicator of inefficiencies in the power market, extremely high prices disproportionately affect consumer well-being, and grid operators face challenges in maintaining grid stability in the midst of large changes in supply and demand. Furthermore, price uncertainty makes investment in low-carbon generation more challenging. Indeed, renewable generation and other decarbonisation efforts have encountered strong headwinds amid a significantly changed market environment. With the simultaneous increase in uncertainty regarding power price levels, accompanied by high investment costs and the highest interest rates seen in a decade, many consumption and generation projects are not reaching final investment decisions or are being scrapped entirely [6]. A lack of new renewable generation via primarily wind and solar, and the slow buildout of flexible, green consumption — such as renewable hydrogen — may open the door for the return of fossil-powered assets when power demand accelerates amid electrification.

Though actors may not be able to fully remedy high interest rates or investment costs, actions can be taken to decrease or reduce the effects, of price volatility. The government can subsidise flexible forms of generation, and TSO operators can improve internal transmission and interconnections to neighbouring zones, which decreases the effect of localised intermittencies in generation. Consumers can engage in load-shifting, i.e., decreasing consumption during high-price periods and increasing consumption during low-price periods. Similarly, producers can utilise flexible generation to increase and decrease production when needed, or by optimising bidding patterns in different electricity markets. Operating in multiple markets with different characteristics can provide significant excess profits compared to the traditional strategy of selling a majority of power via the day-ahead market. Renewable projects may even reach final investment decisions when accounting for these increased market profits. Crucially, the optimised bidding patterns of a single actor are even beneficial from a system perspective, given that in a competitive market price signals provide incentives as to where generation or consumption is most needed in the market.

Thus, the objective of this thesis is to develop a multi-market optimisation stochastic dual dynamic optimisation (SDDP) model for maximising the profit of a Finnish power market company, which operates a renewable power market portfolio consisting of both variable generation and flexible consumption amid price and generation uncertainty. The market portfolio contains two separate wind farms in different locations, a single solar farm and a dynamic hydrogen plant, which converts electricity and water to hydrogen via electrolysis. The created model will operate in three different markets, the day-ahead, the intraday and the manual Frequency Restoration Reserve (mFRR) balancing energy market. In the intraday market, the company will participate in two auctions, intraday auction 1 and 2, which function similarly to the day-ahead auction and have been operational since June 15^{th} 2024. Thus, each hour has four different stages where a decision is made. The created model involves separately optimising the 24-hour period traded for in the day-ahead market. The granularity of the model is on the hourly level with every hour modelled independently of other hours.

This thesis is structured as follows: in Section 2, we provide a deeper context of the Finnish power market, multi-market participation, hydrogen and stochastic dual dynamic programming. In Section 3, we discuss relevant literature and the contributions of this thesis. Section 4 presents the methodology used in this thesis. We provide the rationale for relevant modelling choices and background for relevant data. Furthermore, we describe the formulation of the mathematical optimisation problem constructed to solve the problem of optimal market participation for the agent. Section 5 presents the results in two main subsections: the model outputs for a single use case, as well as a case study to calculate and compare generated profits using the model in six months between January and June of 2024 using the created model and a naive trading strategy. Sections 6 and 7 conclude the work with a discussion on potential limitations and improvements followed by a conclusion.

2 Background

2.1 The European Power market

The objective of this thesis is to optimise trading decisions made under production and price-related uncertainty. To realistically optimise trading in these markets, it is imperative to understand the background of different European electricity markets, especially regarding the typical market behaviour and price formation. Thus, this subsection provides an in-depth description of each of the markets analysed in this thesis. Though this section describes the general European power market, the focus is on the Nordic region, especially Finland.

In Finland, power is typically traded in four main market categories: the financial market, the day-ahead market, the intraday market and Fingrid-operated ancillary markets. The chronological order of the market opening times and closing times is shown in the timeline of Figure 1. The market with the longest-term perspective is the financial market, where derivatives — often futures — of power can be traded. Most often, derivatives traded in the financial market do not include the physical delivery of power, i.e., the contract is purely financial. The futures market is generally used to hedge power market exposure or speculate on long-term swings in market prices [7]. Though the operator of a VPP can, and most likely should, engage in hedging activities in the financial market, we disregard the financial market in this thesis. The motivation for this is the drastic difference in the time frame between the financial market compared to subsequent markets. After the futures market is the mFRR capacity market, which is intertwined with the mFRR balancing energy market. In the capacity market, Fingrid procures reserve capacity per EU regulations. The capacity market is followed by the day-ahead market, which is the market where a vast majority of total power is traded. The intraday market lies between the day-ahead market and the ancillary markets, which operate within minutes before physical delivery.

2.1.1 The Day-Ahead Market

The day-ahead market, often also referred to as the spot market, is the most important electricity market in Europe with regard to market volume. In 2023, the day-ahead market accounted for over 92% of the total traded volume in the Nord Pool electricity markets [9]. Nord Pool is one of the main European electricity market exchanges. It operates across the Nordic, Baltic, UK, Western and Central European markets [9]. The Nordic day-ahead market is part of the European Single Day-ahead Coupling (SDAC) initiative which allows market participants in the Nordic and Baltic regions, the UK and Central Western Europe (CWE) to trade power across borders [10].

The primary objective of the Nord Pool day-ahead market is to find a market clearing price for all participating bidding zones, referred to as an area price. A country can have multiple bidding zones, for example, Norway is split into 5 bidding zones (NO1 - NO5) and Sweden into four bidding zones (SE1-SE4). Typically a country is split into multiple bidding zones due to transmission capacity constraints related to geographical, or other, factors. [11]

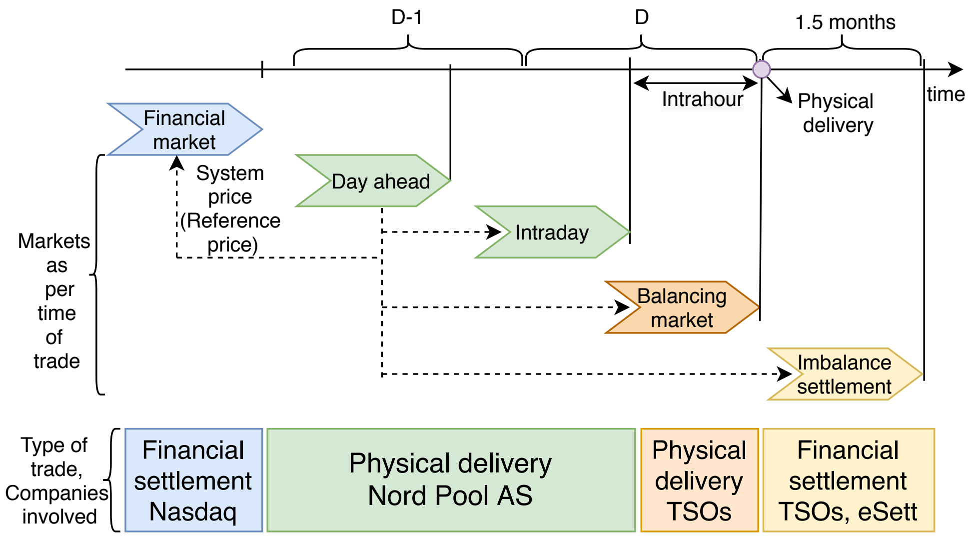

Figure 1: The chronological timeline for trading electricity for a single delivery hour. The figure is from [8].

The day-ahead market functions as a centralised auction, where market participants submit bidding curves at 12:00 D-1, representing the ability to consume or generate power at a certain price point. Each market participant submits bidding curves for each hour. This is referred to as a bidding curve. An operator may also submit block bids spanning across multiple hours in the case that they can not flexibly be powered up or down, however, this is out of the scope of this thesis. According to market regulations [12], each market participant must price sold power according to the marginal cost or the opportunity cost of production. The term opportunity cost refers to the potential benefit lost by choosing one option over another. Figure 2 is an illustration of how the most common generation assets marginal or opportunity costs of the most common generation assets. In general, solar and wind power offer generation at zero marginal cost [13], while coal and gas price generation at the marginal cost derived from emissions and fuel prices [14]. Plants where shutdowns are costly typically offer their generation at the minimum price of -500 €/MWh, as shutting down or restarting the plant generally would cost more than producing power at a negative price.

Crucially, an opportunity cost also refers to the expected value captured in subsequent markets after the day-ahead market. Thus, a generator is allowed to bid less than the maximum available, or forecasted, power into the day-ahead market with the expectation of selling the power in later markets at a potentially higher price. However, this requires that the generator must have a credible expectation for the price of power to be higher in later markets. Furthermore, this power must be bid in subsequent markets. Withholding available power from all markets is against EU market regulations. [12]

Similarly to the supply side, consumers also submit bidding curves for each hour indicating their willingness to consume power at different price points. Ordinary

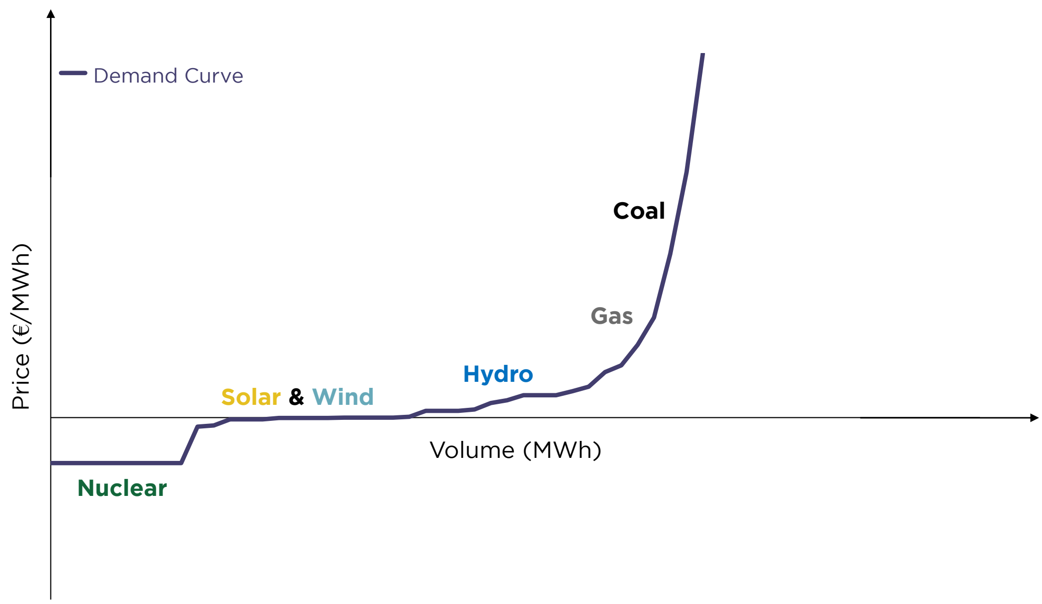

Figure 2: The typical marginal or opportunity costs of different sources of electricity generation.

consumers do not participate in the day-ahead market. Instead, companies selling electricity to consumers make bids based on the predicted consumption at different price points.

After the day-ahead market bidding period closes, all generation and consumption bids are combined into supply and demand curves. The generation bids are organised in a merit order, such that the cheapest bid is at the top of the merit order, the most expensive bid is at the bottom and the bids between them are in ascending order with regards to price [15]. Similarly, the demand curve has increasing demand when the market price decreases. Figure 3 represents a hypothetical merit order for various generation methods.

In a hypothetical day-ahead market consisting of only one bidding zone, the hourly market price would simply be the equilibrium of the supply and demand curves, i.e., the price where the supply and demand curves intersect (Figure 4). However, in reality, the price formation is significantly complicated by transmission connections between different bidding zones and a multitude of different order types in addition to the simple hourly bids explained above. The prices are determined using EUPHEMIA, an algorithm developed for SDAC. The exact workings of EUPHEMIA are out of the scope of this thesis, however, the determination of each bidding zone hourly price is chosen such that it maximises the total welfare, i.e., the sum of the consumer and producer surpluses, and the congestion rent, while simultaneously satisfying transmission constraints [16]. Congestion rent occurs in a situation where two neighbouring bidding areas are decoupled, i.e., have different market prices. In this situation, the total congestion rent is the difference in market prices multiplied by the transmission in the day-ahead market. The congestion rent is paid to the transmission system operators

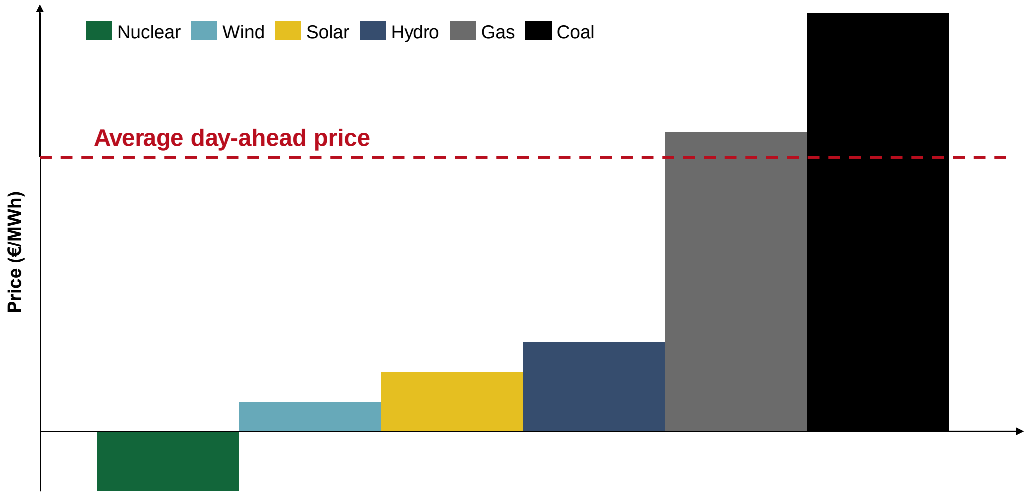

Figure 3: A hypothetical merit order in a bidding zone with nuclear, wind, solar, hydro, gas and coal-powered generation.

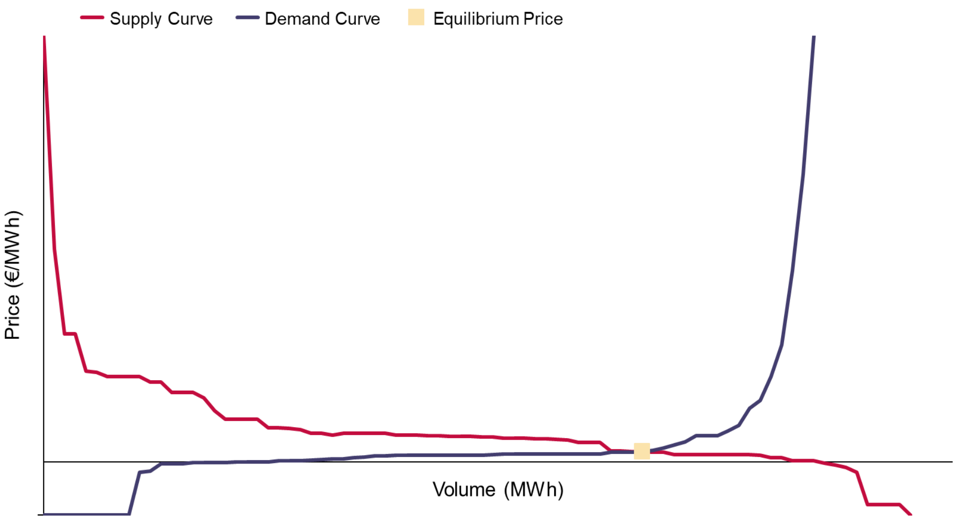

Figure 4: The supply (red curve) and the demand (blue curve) are represented in a Volume - Price coordinate system. The equilibrium price is located at the intersection of the supply and demand curves.

(TSOs) [17].

The resulting market prices determined by EUPHEMIA for each bidding zone are constrained between a minimum of -500 €/MWh and 4000 €/MWh. Market prices in neighbouring bidding zones are the same if the transmission capacity between these zones is not exceeded. If the transmission capacity interconnection is at maximum flow capacity, the prices in neighbouring zones differ.

2.1.2 The Intraday Market

The intraday market opens after the day-ahead market is cleared and its outcome published. In the intraday market, producers and consumers of power can conduct trading in a continuous manner. In Finland, the operator of the intraday market is Nordpool. Nordpool's intraday market consists of 16 countries, encompassing the Nordics, the Baltics and a large portion of the Central European power market, most notably Germany and France [18]. Trading in the intraday market happens between the announcement of the day-ahead market prices and the physical delivery of power. Trades can be made across borders provided the maximum capacity of transmission between the two zones has not been reached. Intraday market trading is done only on a power basis, meaning that different subsidies, guarantees of origin or other external factors do not affect market prices. Trades can be made in different time frames: 15 minutes, 30 minutes or 1 hour [19].

The intraday market is different in many ways from the day-ahead market. Historically, the key difference to the day-ahead market has been the lack of a centralised auction. Instead of combining generation and consumption bids of individual operators to find the intersection of the supply and demand curves, the intraday market prices are determined by a "pay-as-bid" process, which is equivalent to the price formation of the financial stock market: the current market price for the intraday market is determined by the trade price of the previous trade made [19]. Thus, instead of a common area price, intraday prices are characterised by different statistics: typically the hourly volume-weighted average, lowest and highest trade prices. Price spreads between the day-ahead market and the intraday market can often be significant, especially in Finland (Figure 5).

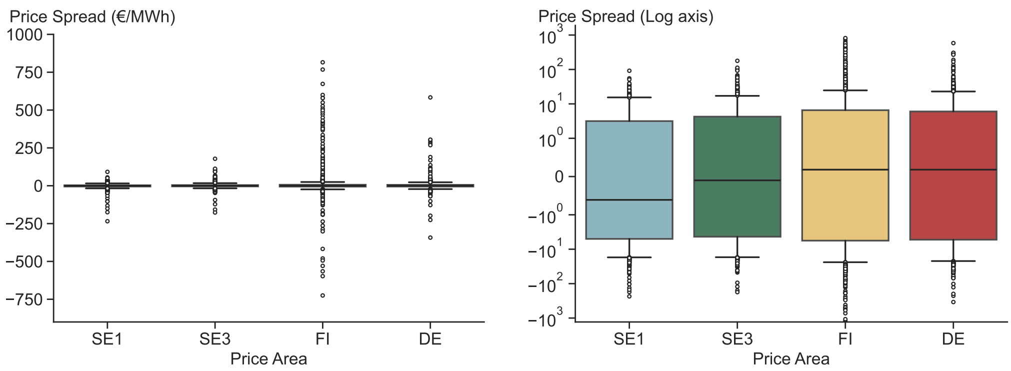

(a) (b)

Figure 5: Boxplots of the price spreads for 2023 (ID volume-weighted average price - spot price) for the Finnish (FI), German (DE) and two Swedish price areas (SE1, SE3). Subplot (a) represents the boxplots with an absolute axis. Subplot (b) has a logarithmic axis.

In addition to the continuous intraday market, Nord Pool introduced three new intraday auctions in June 2024. In this thesis, we refer to these auctions as IDA1, IDA2 and IDA3. The auctions for IDA1 and IDA2 are at 15:00 and 22:00 on the day before delivery (D-1) respectively. Buyers and sellers of power can submit offers for every traded hour. On the other hand, the gate closure for IDA3 is at 10:00 am on the day (D), after a portion of the day has already passed. Thus, trading power in IDA3 is only possible for the period 12:00 - 24:00. Intraday auctions operate on the same fundamental principle as the day-ahead auction. Operators submit their offers, and the EUPHEMIA algorithm solves a market area price which maximises the system welfare in the same manner as the day-ahead market. The only key change to the mechanism is that instead of having full cross-border transmission capacity, only the unfilled or unallocated transmission capacity can be traded in these auctions. [20]

Historically, intraday markets have been used to primarily balance deficits or surpluses of power resulting from the forecasting errors of variable renewable generation. Reducing imbalances in the intraday market before ancillary markets can be thought of as hedging against volatile and uncertain imbalance prices. Balancing renewable energy production is important, as renewable generators submit their day-ahead bids in relation to the day-ahead generation forecast. The intraday market enables the balancing of forecasting errors before the uncertain and volatile balancing market, which not only reduces the market risk of the generator but also reduces strain on the balancing markets [21]. As a large portion of renewable generation also operates in the intraday market, the importance of the market has increased simultaneously with the higher penetration of variable renewables. This can be seen in a significant increase in the total yearly traded volumes between 2012 and 2024 (Figure 6). In 2012, the total yearly volume was 0.5 TW, while in 2024 the traded volume is potentially going increase to over 3 TW.

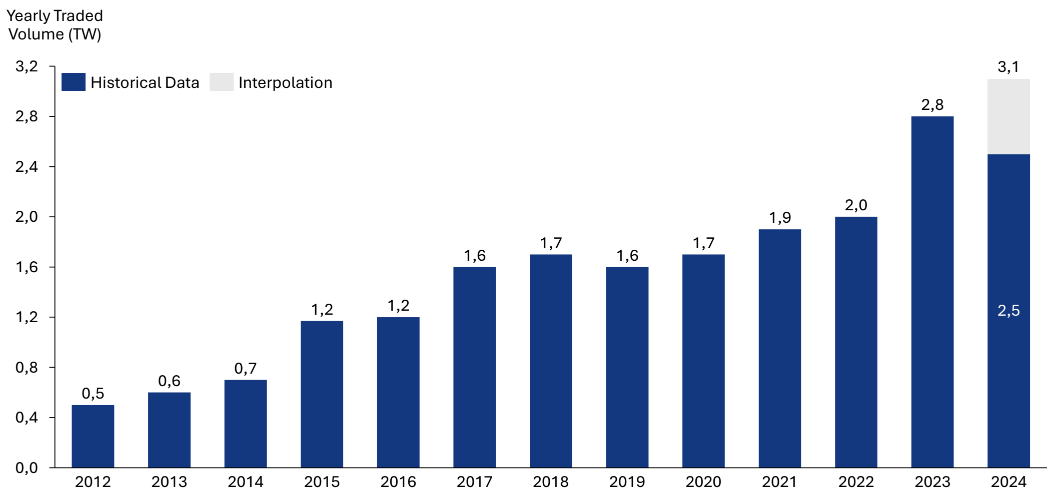

Figure 6: The total yearly traded volume for Finland in the intraday market between the years 2012 - 2024.

As a counterweight to traders attempting to balance power deficits resulting from forecasting errors, intraday markets can bring significant amounts of additional revenue to generators operating flexible generation assets. Typically, the hourly high prices are higher than the corresponding day-ahead price for that hour. Correspondingly, the hourly low prices are cheaper than the day ahead price (Figure 5). Thus, an operator with flexible generation assets might purchase power at a price below their short-run marginal cost if they have committed to producing in the day-ahead market, thus profiting by an amount equal to the difference in MWh between the trade price and marginal cost. Furthermore, producers can also increase output if the trade price in the intraday market exceeds the marginal cost. The opposite is also true for flexible consumption. [21]

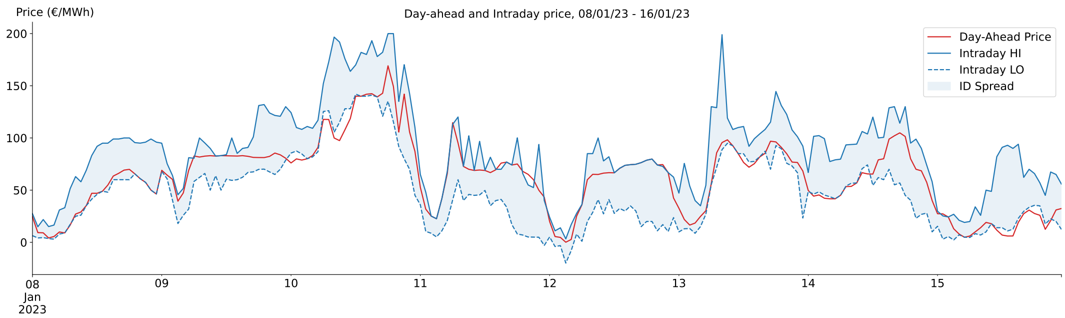

Figure 7: The day-ahead and intraday market prices for the second week of January 2023, with the shaded area in between representing the spread between the intraday high and low prices.

In the context of this thesis, modelling the continuous intraday market presents significant challenges regarding high volatility, random price formation and computational challenges. On the other hand, intraday auctions present an opportunity to include intraday trading in multi-market optimisation, by providing a clearly defined decision point. However, due to the introduction of intraday auctions being so recent, the traded volumes in Finland remain small, which is an obstacle to meaningful modelling of the drivers of price variation between different electricity markets in Finland. Thus, as a proxy with similar functionality to the intraday auctions, we split continuous intraday trades into two different datasets, one for trades made before 18:00 EET D-1 and the other for trades made between 18:00 – 24:00 EET D-1. The used auction price is the final trade price made before the intraday auction period. By making this simplification, we can discretise the continuous nature of the intraday market into singular decision points, simplifying the mathematical approach significantly. Furthermore, this simplification allows the use of data before June 2024 in the analysis of the potential profitability of the constructed multi-market optimisation model.

2.1.3 Finnish Balancing Markets

Transmission System Operators (TSOs) have the increasingly challenging job of constantly maintaining grid frequency, by balancing the supply and demand of electricity. This is a critically important process from a societal welfare perspective. Most electrical grids worldwide operate at a frequency of 50 Hz, and even a 0.5 Hz deviation can put the electricity grid at immediate risk of blackouts [22]. Not only is restarting the grid after a blackout exceptionally challenging, but in the meantime, it also causes significant humanitarian damage, in addition to millions, if not billions, in monetary damages.

Nonetheless, the increase in variable renewable energy has made this task even more challenging. However, TSOs are not without means to maintain grid stability. The Finnish TSO, Fingrid, operates a large number of reserve power plants, which are never operational in a market where regular supply and demand are in balance. They are only turned on when a drop in grid frequency requires them to be used. However, the most important method for TSOs to keep the grid frequency within the required tight limits is via the operation of multiple balancing, also referred to as ancillary, electricity markets. In Finland, the TSO Fingrid operates various reserve markets, which operate at different time frequencies. In addition to differing in the operational timeframe, the markets vary in their role in the stabilising of grid frequency. Figure 8 summarises the different Fingrid-operated ancillary markets and their different activation speeds. In practice, all ancillary markets operate under the same core principles: providers of flexibility offer either up-regulation or down-regulation capacity at a certain price point. Up-regulation refers to an increase in generation (or decrease in consumption), while down-regulation refers to a decrease in generation (or increase in consumption). [23]

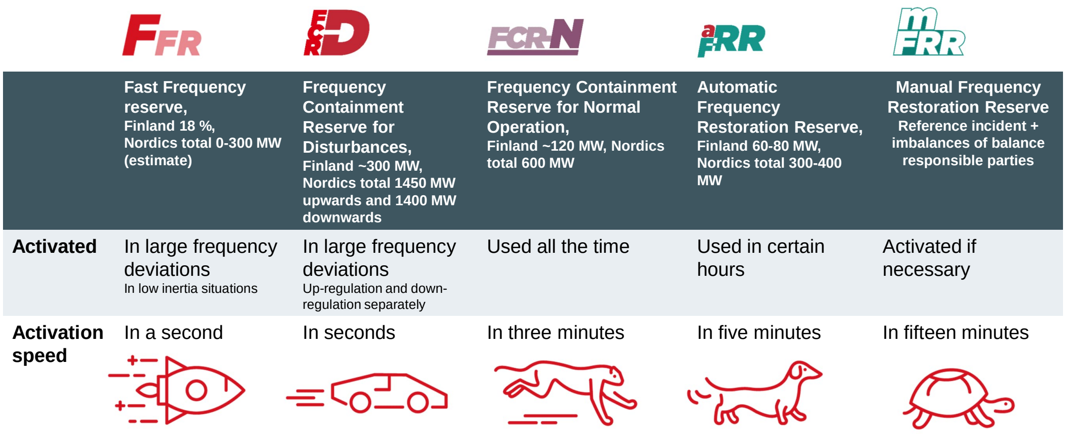

Figure 8: A figure representing all the Finnish ancillary markets. The figure is from [24].

The slowest, and largest, ancillary market is the Manual Frequency Restoration Reserve (mFRR) balancing capacity and energy market. Its primary use is to act as a balancing market in the case of large deviations in supply or demand, for example when a large power plant encounters unanticipated problems. In practice, it operates as two separate markets – the capacity and balancing energy market. The capacity market operates before the day-ahead market, with a closing time of 36 hours before delivery. The capacity market is where Fingrid procures the needed amount of balancing capacity according to Article 3(1) (109) of the System Operator regulation. In practice, the article states that Fingrid must procur reserves totalling the "highest expected instantaneously occurring active power imbalance within an LFC block in both positive and negative direction" [25]. The mFRR capacity market has a market-clearing mechanism similar to the day-ahead market. Flexible generation and consumption submit bids regarding the expected marginal or opportunity cost of an increase or decrease in capacity. These offers are then ranked in a merit order, and the resulting clearing price is the cheapest bid where the supply equals Fingrid's need for flexible capacity. In the capacity market the procured capacity is in power, i.e., megawatts, instead of energy. When a capacity bid is accepted, it requires the producer to submit a bid in the balancing energy market closer to physical delivery. This bid may or may not be activated. If it is, the operator receives both the capacity payment, and the potential balancing energy fee. If the bid is not activated, the producer is still remunerated for the uphelded capacity. In the case of the provider not being able to fulfil their promised capacity commitment, the asset provider is sanctioned by a price of the maximum of the day-ahead and mFRR capacity market price multiplied by three for that hour. [26]

An operator can also only bid energy in the mFRR balancing energy market, which is conducted within 15 minutes of physical delivery. In general, the mFRR balancing energy market is maintained for large variations in supply and demand, for which there is not enough available flexible capacity procured from the capacity market. Thus, in the case of a need for additional generation, Fingrid purchases additional energy from flexible assets. Correspondingly, when there is a surplus of generation, Fingrid sells electricity to flexible consumption or generation. The flexible asset then decreases generation capacity, or in the case of consumption, increases capacity. The mFRR balancing energy has the same market clearing process as the capacity market. However, in this case, the flexible asset is only remunerated for activations. Furthermore, the owner is paid for the total delivered energy, instead of capacity. [26]

Other ancillary markets, in order of time frame, include the Automatic Frequency Restoration Reserve (aFRR), the Frequency Containment Reserve for Normal Operation (FCR-N), the Frequency Containment Reserve for Disturbances (FCR-D), and the Fast Frequency Reserve (FFR). These markets operate between a 5-minute (aFRR) and multiple-second (FFR) time frame. All of these ancillary markets are operated on a capacity basis, meaning that remunerations are based on available capacity or power instead of delivered energy. [24]

One closely related concept to ancillary markets, which is relevant to the agent in the case of this thesis is the imbalance settlement. Imbalance settlements take place after the physical delivery of electricity and involve a payment from the TSO to the agent in the case of an agent surplus, or a payment from the agent to the TSO in the case of a power deficit. The magnitude of the imbalance is the difference between the net commitments in electricity markets and the realised generation. Since November 2021, the Finnish imbalance price has been equal in the case of a surplus or deficit. In Finland, the imbalance price is the maximum price of the mFRR market and the hourly volume weighted average price of the aFRR market. In practice, the imbalance payment can be thought of as the same mechanism as the balancing energy market. However, the key difference is that the imbalance is settled after delivery. In the case of a deficit of power, the operator responsible for the imbalance must pay Fingrid the maximum of the day-ahead price or the up-regulating price, for each megawatt of imbalance. In the case of a surplus of power, the operator receives the day-ahead price or, if the hour is down-regulating, the down-regulating price. The imbalance settlement scheme makes it risky to amount significant deficits of generation at physical delivery, whereas a surplus of generation can easily be curtailed or offered to the grid. [27]

Ancillary markets are inherently random in nature. Modelling the exact price formation is exceptionally challenging without real-time estimates of generation for a majority of power assets. However, analysis in this thesis made for modelling mFRR market prices indicates that some phenomena clearly influence balancing market prices. Similarly to the intraday market, one notable driver of ancillary market prices is renewable generation. Forecasting errors in renewable generation can affect both up- and down-regulation prices [28]. In the case of overforecasting, a sudden drop in renewable generation causes an increase in up-regulation prices. However, renewables can often generate more energy than is forecasted. Though many modern renewable assets have the capability to curtail production, many actors ei ther lack the capabilities or the incentives to do so. This results in a need for decreasing generation, corresponding to down-regulation prices lowering, i.e., it becomes cheaper for actors to purchase power from Fingrid and then curtail their own generation. The exact price point where this occurs depends on the method of generation. For fossil-powered plants, the down-regulation marginal cost is the marginal cost of generation, whereas for VREs the decreased generation becomes profitable when the down-regulation price is negative.

Another key driver of ancillary market prices, also related to the generation of renewable assets, is the availability of residual load. The residual load refers to the demand subtracted by the sum of all zero marginal cost, and nuclear-powered, generation. A negative or low residual load pushes fossil generation out of the merit order, whereas a positive one often results in operational gas-powered assets — or other assets, such as combined heat and power (CHP) assets. In general, when operational these fossil-based assets depress balancing market prices in both up and down directions, due to the increase in flexible capacity in the grid. Other drivers of ancillary market prices are typically more random, for example, unexpected drops in available transmission capacity, or the sudden malfunction of a large power plant. However, many other price drivers exist, which are beyond the scope of this work.

The only ancillary market modelled in this thesis is the mFRR balancing energy market. The reasoning behind disregarding others is threefold. The first and main reason is purely to maintain a tractable computational model. The inclusion of several ancillary markets would increase the complexity and size of the optimisation problem, increasing solving times. The second reason is the above-stated clear correlation between balancing energy market prices and large-scale forecasting errors. This opens the door for the agent in this thesis to operate strategically: does the imperfect correlation between large-scale renewable forecasting errors and inaccuracies in the forecasts for production of the agent's own assets result in it being optimal to over- or under-commit in previous markets? The third reason for modelling only the mFRR balancing energy market is simple: curtailing wind and solar generation is generally a straightforward process. However, the reaction time in older turbines may be significantly slower compared to newer models. Thus, the only ancillary market an older wind farm may be able to operate in is the mFRR market.

2.2 Hydrogen

Hydrogen (H) is the most abundant substance in the entire universe, representing nearly 75% of all standard matter. It is the primary element of all stars, including the sun of our solar system. Although it is the most abundant chemical in the universe, on Earth it is rare in its elemental form. Instead, hydrogen is primarily found as a constituent of water (H_2O) or some other organic material, such as various hydrocarbon molecules [29]. During the past decade, global interest in hydrogen as a source of clean energy for industry and generation alike has surged. Green hydrogen, produced from water using renewable electricity, stands out as a valuable and low-carbon alternative to traditional fossil fuels in typically hard-to-decarbonise processes [30].

Historically, the two main ways to extract hydrogen from water or another chemical compound have been steam-methane-reformation (SMR) and electrolysis. SMR involves producing hydrogen through a reaction of methane, or some other hydrocarbon, and water. It is an emissions-intensive process, as the carbon dioxide produced as a side-product of the reaction is generally released into the atmosphere. SMR is currently the most cost-effective and widely used option for producing hydrogen, representing over 95% of global hydrogen production [31]. The hydrogen produced by SMR is referred to as grey hydrogen, whereas hydrogen produced by SMR together with carbon capture is called blue hydrogen [32].

The alternative to producing hydrogen via emissions-intensive processes is producing hydrogen via electrolysis. Electrolysis is not a new technology. Water was first electrolysed in 1806 by British scientists William Nicholson and Anthony Carlisle. The process occurs in an electrolyser, which contains two electrodes, an anode and a cathode. They are both immersed in an electrolyte, which in the case of hydrogen is water. A chemical reaction is induced when an electric current is passed through the water. At the anode, this causes water molecules to lose electrons and form oxygen gas and protons. At the cathode, protons gain electrons to form hydrogen gas. Hydrogen produced by electrolysis is renewable, provided the electricity used is from a renewable source. We use green hydrogen as a synonym for renewable hydrogen. [33]

Renewable hydrogen provides significant potential for the decarbonisation of heavy transport, which may prove challenging to electrify due to the large distance between destinations. Long travel distances mean that it is unfeasible to utilise a large enough battery for continuous electric transport, meaning that several charging locations would be needed along the way. In the case of flying, the weight of a sufficiently large battery to power long-distance flight would make generating enough lift for sustained flight challenging. Thus, the synthesis of hydrogen into various e-fuels, such as e-methane or synthetic air fuel (SAF), is a potential solution. E-methane and synthetic air fuel are chemically the same compounds as the current corresponding fossil-based molecules, meaning that no new transportation infrastructure is needed, reducing the need for excess investment on behalf of the operating companies. [30]

In the other main usage case, industrial processes are often emissions-intensive, as they typically rely on burning fossil fuels. The use of green hydrogen to replace the burning of these fossil fuels is a viable alternative. For example in the production of green steel, hydrogen is used to reduce iron ore pellets to direct-reduced iron, replacing coke — a form of coal — in the process. This change has the potential to reduce ironmaking emissions by over 95% [34]. In addition to these sectors, hydrogen is often cited to provide an opportunity for other industries to decarbonise. It has been mentioned as an option to store power or as a vital component in ammonia production. However, in all cases, the cost-competitiveness of renewable hydrogen remains to be seen, as the current market, cost and regulatory developments have incurred additional challenges for the rapid deployment of green hydrogen production. [30]

The European Union has defined regulation defining a definition for renewable fuels of non-biological origin (RFNBOs). This legislation is key in defining when hydrogen produced via electrolysis is characterised as renewable, or RFNBO, in the European Union. According to EU regulation, RFNBO hydrogen must fulfil the following criteria [35]:

- **Additionality:** Hydrogen production must not use existing renewable generation.

  "The additionality condition referred to in Article 4(4), first subparagraph shall be considered complied with if fuel producers produce an amount of renewable electricity in their own installations that is at least equivalent to the amount of electricity claimed as fully renewable, or have concluded directly, or via intermediaries, one or more renewables power purchase agreements with economic operators producing renewable electricity in one or more installations for an amount of renewable electricity that is at least equivalent to the amount of electricity that is claimed as fully renewable and the electricity claimed is effectively produced in this or these installations, provided that the following criteria are met:

  (a) *The installation generating renewable electricity came into operation not earlier than 36 months before the installation producing the renewable liquid and gaseous transport fuel of non-biological origin.*

  (b) *The installation generating renewable electricity has not received support in the form of operating aid or investment aid, excluding support received by installations before their repowering, financial support for land or for grid connections, support that does not constitute net support, such as support that is fully repaid and support for installations generating renewable electricity that are supplying installations producing renewable liquid and gaseous transport fuel of non-biological origin used for research, testing and demonstration.*" [35]

- **Temporal and geographic correlation:** Hydrogen should be produced when renewable electricity is available.

  "Until 31 December 2029 the temporal correlation condition referred to in Article 4(2) and (4), shall be considered complied with if the renewable liquid and gaseous transport fuel of non-biological origin is produced during the same calendar month as the renewable electricity produced under the renewables

> power purchase agreement or from renewable electricity from a new storage asset that is located behind the same network connection point as the electrolyser...
>
> From 1 January 2030, the temporal correlation condition shall be considered complied with if the renewable liquid and gaseous transport fuel of non-biological origin is produced during the same one-hour period as the renewable electricity produced under the renewables power purchase agreement or from renewable electricity from a new storage asset that is located behind the same network connection point as the electrolyser or the installation generating renewable electricity, that has been charged during the same one-hour period in which the electricity under the renewables power purchase agreement has been produced. Following a notification to the Commission, Member States may apply the rules set out in this paragraph from 1 July 2027 for renewable liquid and gaseous transport fuel of non-biological origin produced in their territory." [35]

Furthermore, EU regulation lists some exemptions regarding adherence to these criteria. The main exemption concerns two situations regarding the portion of renewable generation in the bidding area, as well as the carbon intensity of the grid. For price areas with a renewable generation of over 90%, producers of hydrogen are exempt from both the additionality and the temporal and geographical correlation requirements. However, the combined production of hydrogen must not exceed the share of renewable generation in the price area. The second condition concerns the carbon intensity: if the grid intensity is less than 18 gCO_{2eq}/MJ, the producer is exempt from the additionality requirement.

In the context of this thesis, we assume that the wind and solar farms in question represent the underlying power purchase agreement (PPA) portfolio for the electrolyser. We assume that the carbon intensity is less than 18 gCO_{2eq}/MJ, which is a roughly realistic assumption regarding the potential Finnish carbon intensity within a few years (the current intensity for 2023 is approximately 25.6 gCO_{2eq}/MJ [36]). Currently, the EU does not recognise electricity from intraday markets as RFNBO. However in this thesis, we assume intraday power to have the same RFNBO percentage as electricity sourced from the day-ahead market. Furthermore, in addition to RFNBO regulation, the EU currently has ongoing efforts to draft regulation concerning hydrogen produced using nuclear power, classified as low-carbon. Both low-carbon and RFNBO hydrogen-derived products are to have a price significantly higher than hydrogen classified as neither. Though the exact interpretation of these regulations is still unclear, the methodology for determining the RFNBO and low-carbon percentage of produced hydrogen is determined by the following logic:

- Available unsold generation of own solar and wind assets is larger than maximum electrolyser capacity → hydrogen is 100% RFNBO
- Unsold generation is less than maximum electrolyser capacity and the remainder of used capacity is sourced from day-ahead market → hydrogen RFNBO percentage is determined by the weighted average of used PPA power (100% RFNBO) and grid renewable percentage (52% for Finland in 2023). The remainder of the produced hydrogen is low-carbon or black hydrogen.

- No PPA generation → produced hydrogen is RFNBO according to grid percentages (52% RFNBO, 92% low-carbon and 8% fossil fuel generation for 2023 on average)

An electrolyser can both be operated in steady and variable states. Steady-state electrolysis is typically utilised in industries where constant hydrogen offtake is needed, such as when producing green steel or when the hydrogen is further synthesised to another molecule, which is typically a less flexible process. On the other hand, flexible electrolysis can significantly enhance the profitability of a hydrogen investment. When operating variably, hydrogen is produced when the power purchased is cheap or the availability of renewable energy is high. This means that flexible electrolysis not only avoids excess costs during periods of high prices but can generate significant excess profits when it is combined with a well-chosen pay-as-produced portfolio. Furthermore, because of a decrease in production during high prices and a corresponding increase during low prices, flexible hydrogen production balances the electricity grid when there is surplus electricity in the grid. This is often the case in countries with a high penetration of variable renewables.

There are multiple different types of electrolyser technology. The main three are alkaline, photon exchange membrane (PEM) and solid oxide electrolysis (SOEC). All these technologies have different ramp speeds and shutdown times. However, the most flexible alkaline and PEM electrolysers can alter output in minutes, or even seconds. This makes it suitable for operation in multiple markets. [37]

In the case of this thesis, we include a dynamic PEM electrolyser producing hydrogen according to market price signals. It can ramp production up or down within minutes without constraints and the incurred ramp-down cost is assumed to be negligible. It has a minimum capacity of 0 MW and a maximum capacity of 60 MW. We disregard downstream processes such as the synthesis of the produced hydrogen to another molecule, and challenges in the offtake of dynamically produced hydrogen. The focus is purely on power market optimisation. Though this approach may not be fully realistic and practical from an industry standpoint, the objective is to demonstrate the potential for a flexible electrolyser in power markets.

Utilising an electrolyser in this fashion can provide significant additional value for the agent. It enables the implementation of riskier trading strategies by acting as a fail-safe for the agent: in cases where there is a large surplus or deficit of power, instead of selling it to the market, the operator can decide to increase or decrease electrolyser output: the worst case result is only encountered if the imbalance exceeds the room for flexibility in the electrolyser. Thus, strategies where the agent buys a large excess of electricity in earlier stages with the intention of potentially selling it for a higher price in a subsequent market is a valid strategy, because the electrolyser is hedging the market risk.

2.3 Stochastic Dual Dynamic Programming

This thesis uses stochastic dual dynamic programming (SDDP) to optimise the bidding strategy of an agent operating a power portfolio in multiple power markets. The problem can be formulated as a multi-stage optimisation problem with stagewise stochastic elements. In this section, we briefly present the main basic concepts and theory required to understand the implemented SDDP model. The SDDP-related methodological concepts outlined in this section are based on [38] and [39].

In multistage stochastic optimisation problems, an agent makes decisions which affect the state of the system over time. Each decision point is referred to as a node. The term node is generally synonymous with the term stage, however, we use node as there can be multiple different nodes at a certain point in time. Indeed, the model formulated in this thesis has multiple nodes for each stage. At each node, the modelled agent makes a decision affecting the state, i.e., the current situation, of the system. This decision is referred to as a control variable. A control variable is denoted by the letter u. Similarly, the state of the system is tracked from node to node by a set of state variables. Each state variable represents a property of the modelled system. The incoming value for the state variable is denoted as x, whereas the outgoing variable is denoted as x'. For example in the case of a milk producer, a control variable could be the amount of powdered milk sold to the market for each node t. Thus, one logical state variable would be the cumulative amount of sold milk during the entire year.

In addition to state and control variables, an inherent property of stochastic multistage optimisation problems is the presence of random elements. We refer to the stagewise stochasticity as random variables. An example of a random variable from the perspective of the same milk producer in the previous paragraph would be the total amount of rain in millilitres for a week t. Possible realisations of random variables are denoted by ω, which are drawn from the sample space Ω. In SDDP, random variables can be the same for each node, or they can be node-dependent.

At any node i, the three variables discussed above are connected by a transition function. The transition function links the incoming state variable x, the chosen control variables u_i and the random variables ω by the function $x' = T_i(x, u, \omega)$. When the agent enters a node i with the initial state x, it selects the control variables such that the stagewise cost function, or in the case of this thesis the stagewise profit function, $C_i(x, u, \omega)$ is minimised.

Control variables are chosen by the agent with a decision rule $u = \pi_i(x, \omega)$, which links the incoming value of the state and the realisation of the random variable to the chosen control. The chosen control is constrained by a set of constraints, denoted by $U(x, \omega)$. Figure 9 is an illustration of how the incoming state and realisation of a random variable are mapped to an outgoing state by a chosen control.

Each node is related to each other by a policy graph, which represents how each node is connected. There can be multiple types of policy graphs - a linear policy graph refers to a connected graph with only one node per stage. On the other hand, a Markovian policy graph is a graph with multiple nodes for each stage. Each node i of a stage in time t has a certain transition probability to transition to another node j at time $t + 1$. Additionally, policy graphs can have cycles, which allows the modelling of a problem with an infinite horizon. Figure 10 is an illustration of a Markovian policy graph with two distinct states. This thesis also models the multi-market problem using a Markovian policy graph, however the number of states is significantly larger.

In the case of a policy graph with more than one node per decision point, the nodes

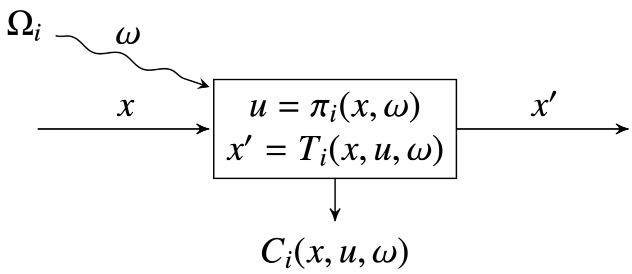

Figure 9: A diagram representing how the controls, incoming state and outcoming state are connected by the transition function. Source [39].

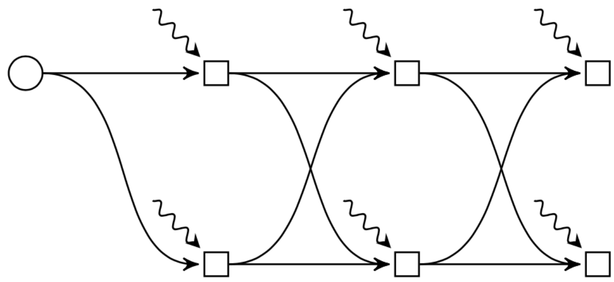

Figure 10: A policy graph representing a Markovian policy graph with two different Markov states. Source [39].

are related to each other by a transition matrix. The transition matrix represents the probability of transitioning from one node to another when moving from time t_{t-1} to time t.

In SDDP, the goal of the agent is to reach a set of optimal decision rules for each stage, i.e., the set of decision rules minimising the expected cost (or maximising the expected profit). A set of decision rules is referred to as a policy. Thus, the optimal decision rules are referred to by the term optimal policy. The optimal policy is reached by minimising the expected cost when starting from the root node with an initial condition x_R. From there, the agent moves from node to node along probabilistic paths until reaching the "zero" node, i.e., a node without any outgoing probability arcs. Thus, the function to be minimised for a problem with i stages is of the form

$$\begin{aligned}\mathbb{E}_{\omega_1 \in \Omega_1} \Bigg[\min_{u_1} \Bigg\{ C_1(x_1, u_1, \omega_1) + \mathbb{E}_{\omega_2 \in \Omega_2} \Bigg[\min_{u_2} \{ C_2(x_2, u_2, \omega_2) \\ + \mathbb{E}_{\omega_3 \in \Omega_3} \Bigg[\min_{u_3} \{ C_3(x_3, u_3, \omega_3) + \mathbb{E}(\ldots) \} \Bigg] \Bigg\} \Bigg] \Bigg\} \Bigg]\end{aligned} \tag{1}$$

The SDDP algorithm operates through two distinct phases:

- Forward pass: in the forward pass, scenario realisations are sampled sequentially from the initial stage to the final stage. For each state, approximate subproblems are solved using the cost-to-go function. The cost-to-go function is approximated from the cutting planes of previous iterations.

- Backward pass: in the backward pass, the cost-to-go function approximations are improved by incorporating new cuts into the subproblem, by following Kelley's algorithm. Given that the cost-to-go function is assumed to be convex concerning state variables, this results in an under-approximation of the true minimum cost-to-go (and thus the overall optimisation function). [39]

The combination involving a forward and backward pass refines a lower bound for the solution iteratively. After completing the iteration, an upper bound for the policy is estimated by sampling the scenario space and solving related problems with the cost-to-go function updated during the earlier iteration. The algorithm continues until it reaches convergence, or until the desired number of iterations is achieved. This thesis uses an implementation of SDDP called SDDP.jl, which is a package for solving stochastic dual dynamic problems in the Julia programming language. [38]

3 Literature Review

3.1 Research on Optimal Energy Market Strategy

Historically, the European power sector was vertically integrated and monopolised, with only a handful of companies responsible for the generation, transmission and distribution of produced power generators. Thus, there was no need for the widespread trade of power. However, electricity markets underwent gradual liberalisation during the 1990s, first beginning with the liberalisation of the Chilean power market in 1980 [40]. The liberalisation of the European power market resulted in the day-ahead market, which remains the market where a majority of produced electricity is traded. Already in the 1990s, it was shown that in an efficient day-ahead market auction it is always optimal for a generator to bid at their known marginal cost [41]. However, power markets have developed significantly since then. In the Nordics, a generator can operate in as many as eight power markets, each exhibiting different behaviour and market price formation mechanisms. According to European Union regulation REMIT article number 5, a generator may price power differently to the marginal cost if they have a "reasonable economic, technical or regulatory justification for not offering the capacity, or offering it above marginal cost". Generally, an opportunity cost is considered a reasonable economic justification. Thus, in a setting with multiple markets, a producer may, and should, price power according to the expected profit available in subsequent markets after that market. Furthermore, uncertainty in renewable generation is also a valid justification. Therefore, instead of a singular power market where a generator with full control of its assets can sell power, a modern producer of power must consider both the uncertainty regarding variable power generation, as well as the opportunity cost of making decisions in a market, given potential price developments in subsequent power markets. [12]

In this thesis, the modelled power portfolio consists of two wind farms, a solar farm and a dynamic electrolysis unit. In the literature, a portfolio consisting of multiple different assets is generally referred to as a virtual power plant (VPP). The optimal bidding strategy of a VPP has been researched in multiple studies using various methods and with a focus on both single or multiple power markets. For example, [42] and [43] optimise the day-ahead patterns of a VPP using two different methods. In [42] the cost of a VPP consisting of renewable generation and a battery storage device under demand, price and generation uncertainty is minimised by using a meta-heuristic optimisation algorithm. On the other hand, [43] proposes a bilevel optimisation framework to optimise market profits, which is then transformed into a mixed integer linear programming problem.

In addition to trading power in the day-ahead market, this thesis also takes the intraday and balancing markets into account. Trading of a VPP, or often a singular power storage unit, in intraday electricity markets can modelled with various different approaches [44, 45, 46]. Using a similar methodology to this thesis, [44] and [45] model the optimal participation of a VPP comprising of wind, hydro and thermal power in a cross-border continuous intraday market using a multistage stochastic integer programming problem. The resulting problem was solved using stochastic dual dynamic integer programming (SDDiP). The research shows that risk aversion and available transmission capacity affect potential profits for a VPP in continuous cross-border markets. Similarly, [45] uses SDDiP to model the trading of a VPP consisting of wind, hydro and thermal units in two different order clearing methods. On the other hand, continuous intraday trading of a battery storage unit was modelled using a deep reinforcement learning framework by presenting the decision-making as a Markov decision process.

In [47], the trading strategy of a VPP consisting of only intermittent renewable energy sources is optimised using a portfolio allocation strategy for splitting forecasted renewable generation across day-ahead and intraday markets. The authors find that the proposed portfolio allocation method would have resulted in an improvement of 20% in profits generated from the European Power Exchange (EPEX). In a similar study, [48] show that a wind power producer can substantially increase revenues by participating in the intraday market by using a simple algorithm considering intraday trade prices and forecasted up- and down-regulation prices. The authors also show that revenues are dependent on the market liquidity of the Elbas intraday market, which is the predecessor of the current cross-border intraday market.

Many research studies also take potential balancing market revenues into account. The authors in [49] find the optimal scheduling strategy for a VPP in day-ahead and balancing markets by modelling the VPP as a price taker. Focusing on the optimal offering of a VPP for maximisation of day-ahead profits while simultaneously minimising imbalance costs, [50] shows that a stochastic bi-level optimisation for offering strategy increased VPP profits by nearly 5% in the Greek power market in 2016. A common theme for most balancing market analyses is the incorporation of renewable generation-related uncertainty in the optimisation of the VPPs offering strategy [51], [52]. The authors in [53] present a multistage approach for the optimal bidding of variable renewable energy in day-ahead, intraday and balancing energy markets in the Iberian electricity market. The authors use a linear programming (LP) formulation to solve the optimal bidding strategy of a VPP aggregating wind, solar and a battery system. The added value of participating in all markets analysed is shown to be 10.1% in 2022.

In studies concerning the optimal offering and trading strategies of a VPP, the VPP often consists of some form of intermittent renewable generation some type of energy storage or consumption application as well as potentially a hydropower or thermal power plant. In the case of the VPP modelled in this thesis, the component of the VPP capable of consuming power is the dynamic electrolyser. Optimising market trading strategies for an electrolyser is a less widely documented phenomenon. Though the optimal control of an electrolyser has various existing studies, these often have a primary focus on the physical restraints of the electrolyser instead of maximising electricity market profits. For example, articles concerning optimal electrolyser control [54], [55] and [56] all consider a setting where electricity prices are known before deciding the electrolyser production schedule, which is inapplicable for the setting of this thesis, as it involves four auction processes where prices are unknown at bidding times.

3.2 Relevant Applications of SDDP

Stochastic dual dynamic programming was first presented as a methodology for solving multistage stochastic optimisation problems in 1991 by [57], who demonstrated its effectiveness by obtaining the optimal scheduling of a 39-reservoir hydro valley. Since then, it has been widely used in different energy optimisation problems ranging from energy expansion problems to the market optimisation of VPPs in multiple markets given stochastic elements regarding price or production uncertainties. In this subsection, we survey relevant research concerning problem applications similar to the problem of this thesis, with a focus on how the various stochastic elements are modelled and solved.

A majority of optimal offer strategy research using SDDP concerns the optimal dispatch of pumped hydro or other storage resources. For example, the authors in [58] apply SDDP to a hydrological facility amidst multiarea renewable production uncertainty. The authors present a multiplicative autoregressive process to model renewable generation uncertainty. The alternative to modelling generation uncertainty with an autoregressive process is via discretising the uncertainty into different Markov states or by a scenario tree generation. For example, [59] models the optimal scheduling or a renewable energy-based park power system using SDDP, where uncertainties are discretised into Markov chains with different transition probabilities.

Modelling of price-related uncertainty using SDDP can also be modelled either by discretising the price into different Markov states or by modelling the price process as an autoregressive process. The authors in [60] present a new algorithm for solving multistage stochastic programming problems with stochastic elements within the objective function, which does not require discretisation of the price process. They show that the algorithm converges with near certainty, and demonstrate an application for the algorithm in a hydro-bidding example by modelling the day-ahead price process using an autoregressive process. However, modelling the price process in this fashion has several drawbacks. In the case of this thesis, the main drawback is the independence of the price process to all additional variables in the model [61]. In [62], the decision process of a dairy farmer in New Zealand is optimised over a year-long period, with the objective function uncertainty regarding prices modelled as a scenario tree describing a stochastic process.

3.3 Thesis Contribution

As stated in the previous two sections, a significant amount of research has been conducted concerning the optimal participation of a VPP in multiple electricity markets. This thesis contributes to this research by developing a multi-market strategy optimisation model for optimising the bought and sold volumes of power for a VPP. However, in contrast to other studies and due to the relative novelty of intraday auctions, this thesis is one of the first models combining intraday auction characteristics to optimise optimal trading strategies in the intraday market. It is most similar in nature to [53], which focuses on the Iberian power market. Furthermore, the techniques for scenario generation techniques are similar in nature, employing clustering techniques to categorise large amounts of simulated data points into representative scenarios. This is still noteworthy, as a problem setting with a combination of a day-ahead market, the intraday market, as well as a balancing energy market, has not gained much attention in earlier research [63], especially in a Nordic context. Furthermore, in contrast to studies examining the optimal control of an electrolyser, such as [54], [55] and [56], the problem formulated for this thesis is a setting where price realisations are observed only after deciding the electrolyser capacity. The inclusion of a perspective including the value of RFNBO-certified hydrogen is also a noteworthy contribution.

4 Modelling Foundations and Mathematical Formulation

This work examines the benefits of trading with a VPP in multiple power markets, at discrete time points, with a combination of two wind farms, a solar farm, and a dynamic hydrogen facility. We assume the generation assets function as a PPA portfolio for the electrolyser. This section presents the methodological component of this thesis: the exact methods in creating the underlying assumptions and predictive models used as inputs for the SDDP model, the SDDP model itself, and the derivation of meaningful results from the output policy of the model.

The objective of this thesis is to find a coordinated trading strategy for a VPP trading in the day-ahead, intraday and mFRR balancing energy markets, that is operating under generation and price uncertainty. The problem is modelled by considering a policy graph representing the possible observable states the agent can be in at a certain point in time. An example policy graph for the model is presented in Figure 11. It represents a simplified variant of our model, containing only 10 states per final three stages instead of 80.

Starting at the root node on the left, the decision-making progresses to the first stage, the day-ahead market. This stage is divided into two separate consecutive nodes $t_{1,1}$ and $t_{1,2}$, the reasoning for which will be discussed in Section 4.2. After the day-ahead market, the agent must decide on controls for the first intraday auction, followed by the second auction. The intraday auction stages each have 80 different nodes, or states. These states represent different realisations of forecasted generation for the agent's own generation assets. Additionally, each state has an associated price level. After the intraday auctions, the producer makes their final decision in the mFRR balancing energy market. Similarly to the intraday market, this stage is also divided into the same 80 separate nodes as in previous stages. However, in addition to having the same associated price and production values, each state also has an associated binary variable, representing if the state in question is up-regulating or down-regulating. The exact methodology for determining the characteristics in these states is discussed in Section 4.2. Each hour is examined independently from the perspective of the model, meaning that the policy graph is unique for each hour.

Thus, to meaningfully model the setting of the agent in this problem, one must be able to quantify three sources of uncertainty: the price, production and market volume-related uncertainties. Therefore, in this section, we present the methodology behind uncovering the relevant characteristics of these uncertainties. First, we present a short description of the computational setup. Sections 4.2 and 4.3 present the modelling choices for price and production-related uncertainty. After presenting the sources of uncertainty, we present the resulting mathematical formulation of the SDDP model.

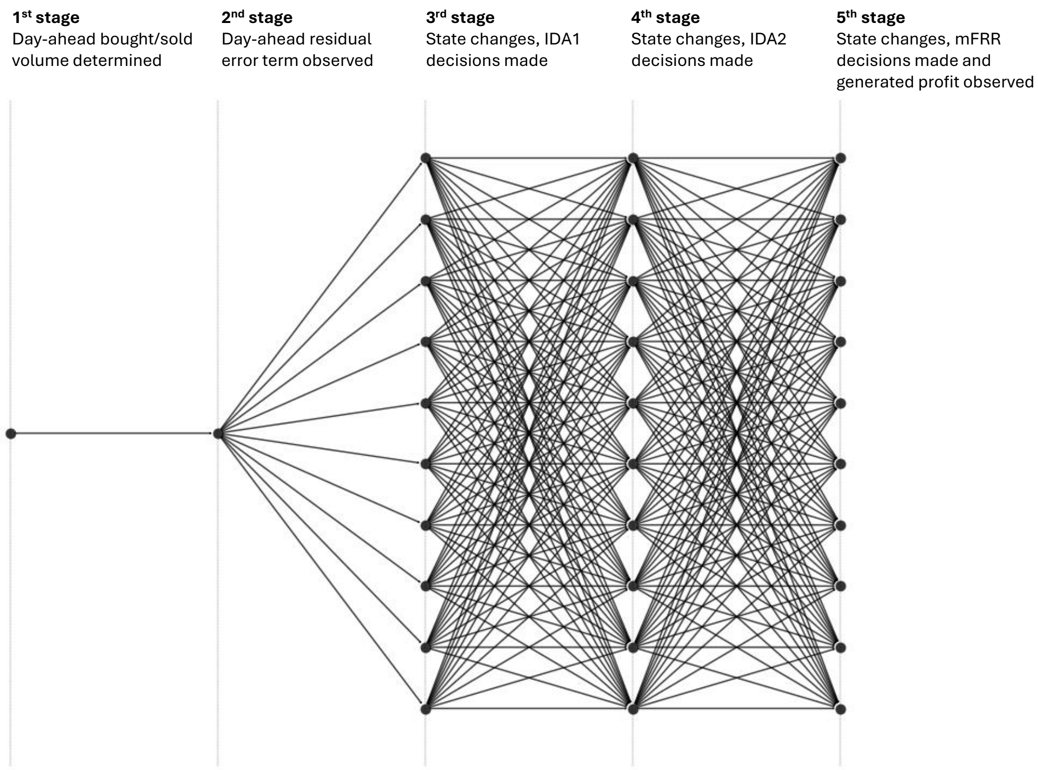

Figure 11: A simplified policy graph of the modelled problem. The circles represent nodes and the lines represent transition probabilities between the two nodes.

4.1 Computational Setup of the Problem

The problem modelled in this thesis is analysed using two different programming languages. Furthermore, the two main phases of the modelling workflow are executed in two different computational environments.

The first phase of the modelling workflow involves the simulation of the SDDP model states and transition matrix — referred to as the data generation phase — passed as inputs to the SDDP model. This phase is executed in a local setting using the Python programming language (Version 3.12.2). One iteration, representing one hour, takes approximately 5 minutes on a laptop with a 1.4 GHz 12-core Intel Core Ultra processor and 16 GB of RAM. This process is parallelisable, as each hour is independent of other hours.

The second phase concerns solving the optimal policy for each hour using SDDP. The model is created using the SDDP.jl modelling framework [38]. Furthermore, the random elements of the model utilise the Distributions.jl package [64]. It is solved in a Julia environment (Version 1.11.1) using the Gurobi optimiser (Version 11.0) [65]. A single hour of the solution can be obtained in a local setting in approximately 3 - 10 minutes, depending on the individual characteristics of the hour in question. Additionally, the maximum amount of iterations is set to 4000.

It is computationally infeasible to obtain all the solutions in a local setting in a reasonable time when validating the results across a period spanning the first half of 2024. Thus, in this case, all solutions were obtained using computer resources within the Aalto University School of Science "Science-IT" project. In using these resources, obtaining solutions was parallelised to use multiple CPUs per task in multiple nodes. Thus, the total solution time was less than 6 hours

The main intended usage application for the model presented in this thesis is to determine optimal strategies for the entire 24-hour period traded for in the day-ahead market. As the model workflow can be parallelised, solutions for the next 24 hours can be obtained within 30 - 45 minutes. Though this is close to the upper limit of solution time for an agent making decisions in these markets, it is still rapid enough to remain suitable in assisting decision-making.

4.2 Market Price and Volume Uncertainty

4.2.1 The Day-Ahead Market

The first decision made by the agent is the amount of volume sold or purchased in the day-ahead market. The day-ahead market has a modelling approach that is significantly different from subsequent stages. In the day-ahead market, the agent is assumed to be a price-taker. Thus, any control decision regarding bought volume does not affect the eventual price level from the perspective of the producer. It can purchase or sell as much power as possible, with some practical restraints to restrict trade volumes within acceptable limits from a risk perspective. These stagewise constraints will be presented in Section 4.5.

In addition to being the only market stage with no market volume-related uncertainty, the day-ahead stage is the only part of the model which uses an external price model prediction. This prediction is a time series model originating from the SKM Market Predictor platform [66]. It has hourly data granularity, i.e., it has one market price prediction for each hour. The specific forecasted model was chosen by comparing the mean-squared errors of 15 different time series models for 2023 and choosing the best-performing model.

Each day-ahead price forecast of the chosen model has a randomly distributed residual. Thus, in the day-ahead stage of the model, the stagewise random variable is randomly sampled from the distribution of empirical residuals of the forecasting model. The distribution is chosen by fitting a distribution to the data using the Python Fitter package [67]. The best fitting distribution is the Cauchy distribution, with parameters $(\mu \approx 0.81, \sigma \approx 1.4)$. To keep the model from becoming too large, only 30 values are sampled from the distribution for the model to randomly sample one from in the decision-making process.

SDDP.jl handles any stagewise-dependent uncertainty, i.e., a random variable within the model, as a hazard-decision subproblem. The term hazard-decision refers to the agent first observing the realisation of the random variable, after which the agent makes a decision. However, this is not realistic in the case of a producer bidding in day-ahead markets, where the realised price is observed after making the bidding decision. Thus, to make the stage a decision-hazard instead of a hazard-decision subproblem, the day-ahead market stage is divided into two separate nodes $t_{1,1}$ and $t_{1,2}$. In node $t_{1,1}$ the agent makes a deterministic decision without any stochastic elements based only on the forecast for the day-ahead price (in addition to other relevant variables). In node $t_{1,2}$, the producer observes the realisation of the random variable, i.e., the percentage error sampled from a distribution of empirical residuals. The decision made in this node is constrained such that it must be the same as the decision made in the earlier stage. Thus, no actual decision is made in node $t_{1,2}$, instead, the hazard-decision subproblem is converted into a decision-hazard one. In a later context, we refer to these two separated stages collectively as the day-ahead stages.

4.2.2 Intraday and mFRR Balancing Energy Markets

Price and volume-related uncertainties are modelled differently in the three remaining stages. However, all three stages are quantified using a similar methodology. Additionally, the final mFRR stage has a minor methodological addition concerning market uncertainty. The price uncertainty in these markets is modelled using 80 unique representative states. Each state has six relevant metrics from the perspective of the model: the forecasted market price (€/MWh) and the forecasted generation (MW) of the two wind farms and one solar farm operated by the agent. Additionally, each state node contains a value for the forecasted macrolevel wind and solar generation. Furthermore, in the mFRR ancillary market binary variables are associated with each state depending on if the state is up- or down-regulating. The volume-related uncertainty — representing the maximum capturable market volume — is addressed by sampling from a distribution for each of the final three stages in the SDDP model.

The maximum capturable market volume is the more simplistic of the modelled uncertainties in this stage. We include a stagewise random variable in the model as a proxy to represent the amount of capturable liquidity in the market, which is assumed to be randomly distributed. Furthermore, the distributions for the market volume are separate for every hour and every market, as often traded volumes are significantly higher during peak times and in timeframes closer to delivery. The distributions are obtained by using the Python Fitter package to fit distributions for each hour. The data used for the intraday market stages is the cumulative trade volumes in the continuous intraday market for each delivery hour, in the time between each stage. This decision is motivated by the lack of trading volumes in the intraday auctions in the present, as discussed in Section 2.1.2. Figure 12 illustrates the data and fitted distributions for hours 05:00 (a) and 20:00 (b) in the three considered markets. Each SDDP iteration samples a value from the fitted distributions for each market stage. The sampled values are then multiplied by a constant scaling factor of 0.15. Some of the fitted distributions have a non-zero probability of obtaining values nearing infinity. Thus, we limit the value of the maximum capturable market volume to be at most 125. The obtained market volume represents an assumption regarding the possible capture of market volume, while still assuming that the agent's actions would not affect the price of the market. As this thesis has no information available regarding the market sensitivity of the auction setting, 15% is assumed to be the standard assumption, which is deemed realistic for a large operator in Finland.

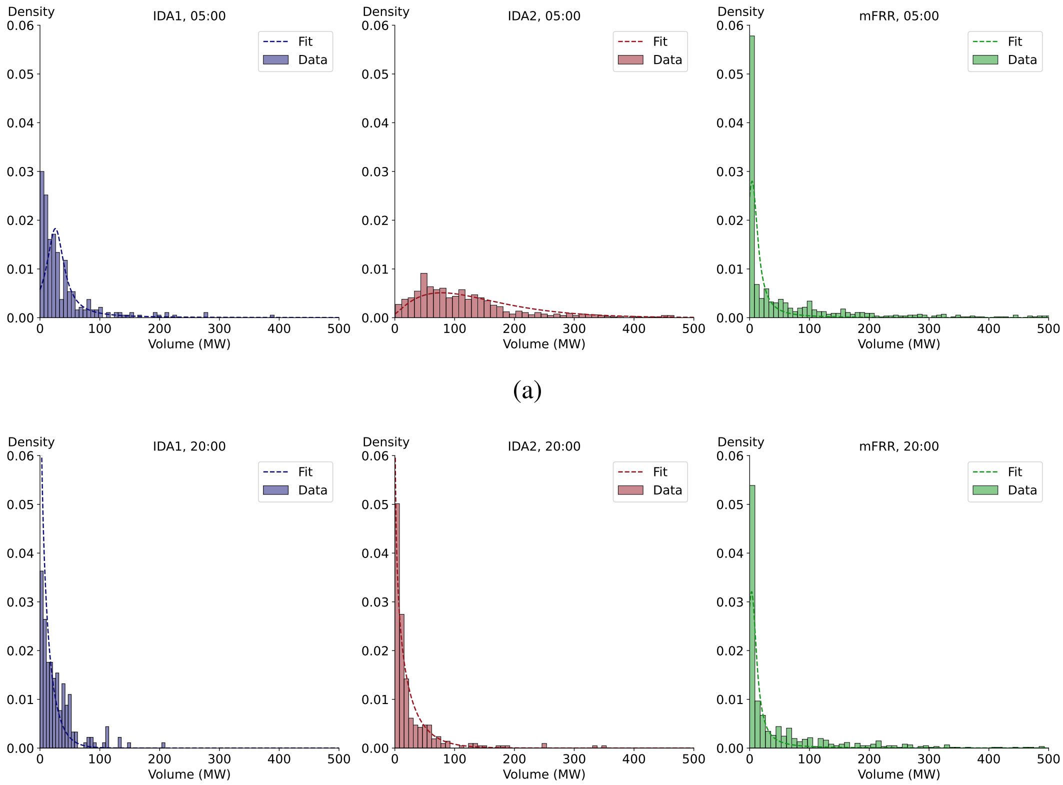

(a)

(b)

Figure 12: Fitted distributions and data for market volume in the IDA1, IDA2 and mFRR stages for 05:00 (a) and 20:00 (b).

The market prices for each state are obtained by simulating 2000 iterations of a stochastic process, which progresses from the day-ahead stage to the mFRR stage. The primary random elements are the large-scale forecasting errors concerning wind and solar. Furthermore, these forecasting errors are correlated with the generation of the agent's assets. The stochastic process has a price variable, which is obtained by predicting the change in price level from the previous price, given the random change in forecasted generation. The resulting prediction for the market price of each stage in the 2000 iterations is obtained by training an Extreme Gradient Boosting (XGBoost) regression model using historical data from 2023 until August 2024.

The XGBoost model for each intraday auction stage considers twelve features for each hourly data point, some of which were listed as price variation drivers in Section 2. The mFRR price model is given only eight features. For all models, the main features are the changed wind forecast W_F from stage *t-1* to *t*, the forecasted residual load R, and the price P_{t-1}. Furthermore, we include three temporal variables to capture the different behaviour on an hourly, daily and monthly level, as well as the allocated transmission to neighbouring price zones after the day-ahead market. The mFRR model has the same features, however without the transmission constraints, and with the solar forecasting error included as an additional predictor. The label for all three models is the market price for the current stage P_t. The models were trained using a training split of 90/10, a learning rate $\lambda = 0.1$ and 100 estimators with a maximum depth of 5.

The wind forecast data for each stage, provided by Fingrid, represents the forecasted wind power at 15:00 D-1 for IDA1, and 22:00 D-1 for IDA2. In these two auctions, the power is traded for the entire 24 hours of the day in question. Thus, the accuracy of each forecast is different due to different proximities to physical delivery. Therefore, the stochastic element is sampled 24 times, for each hour, from a distribution fit using the historical data for the corresponding hour at 15:00 and 22:00. As stated in the previous section concerning intraday auctions, we do not use actual intraday auction data for the price forecasting, or modelling. Instead, the used metric is the final trade made before 15:00 D-1 (EET) for IDA1 and 22:00 D-1 (EET).

The most satisfactory model accuracy was seen for models concerning the final trade prices for IDA1 and IDA2. They achieve R-squared values of 0.93 for IDA1 and 0.92 for IDA2 (Figure 13(a) and 13(b)). On the other hand, in the prediction model for mFRR, the balancing energy forecasting was less satisfactory (Figure 13(c)), achieving an R-squared score of approximately 0.54. However, this is unsurprising, as markets with shorter time periods until delivery often exhibit a wider variety of random elements, making sufficient modelling challenging. All subfigures in Figure 13 contain a sample of the first 75 model predictions plotted against the corresponding test set.

Possible decisions made in the mFRR market are primarily determined by the current needs of Fingrid for the increase, or curtailment, of power. The simultaneous purchase and sale of power on behalf of Fingrid in the mFRR market is not possible during the same market period. Every hour can be one of three: up-regulating, down-regulating or neither. However, in the SDDP model, the residual of the spot price is observed within the model, meaning it is challenging to infer the mFRR state inside the model, as this would require tracking the residual of the day-ahead price forecast and comparing it to the mFRR state price forecast. Thus, to account for the uncertainty regarding up- and down-regulation states, without tracking the realisation of the random day-ahead price within the model, we separately determine two binary variables r^+ and r^-. These binary variables are included in each subproblem's stagewise objective function, where they determine if the agent is able to sell or produce power for that corresponding state. They are given as inputs to the SDDP model.

The binary variables for each state were determined using a random forest classification model, a common supervised learning-based model used for classification tasks. As the classification was performed outside the SDDP model, only data available at the root node or when making mFRR decisions was used in the training phase of the model. The features of the model are thus the day-ahead price forecast, and the change in wind and solar forecasted at the day-ahead decision compared to the actual production (assumed to be equal to the forecast at the mFRR decision). Additionally, the hour, day, month and forecasted residual load are included as features. Training data was available from the beginning of 2023 until August 2024. The label of the classification model was determined based on the realised day-ahead prices:

- *mFRR price > Day-ahead price → Upregulating*
- *mFRR price < Day-ahead price → Downregulating*
- *mFRR price = Day-ahead price → Neither*

The trained classification model has a test set classification overall accuracy of approximately 0.70. The precision, recall and f1-scores are all 0.74 or higher for down-regulating hours (Table 1). For up-regulating hours, the precision, recall and f1-scores are slightly lower but remain above 0.7. The poorest classification performance is in the case of hours which are neither up- or down-regulating. The lower classification scores for up-regulation hours compared to down- may be caused by the extent of the training data, which only extends from January 2023 to June 2024. Spring and summertime tend to be more common for down-regulation, whereas up-regulation is more common during winter. Thus, the training data has more realisations of down-regulation than up-regulation hours.

From the perspective of power markets, the most costly classification error for the agent is when up-regulation hours are mistakenly classified as down-regulation hours. This classification could result in larger-than-ideal power deficits, potentially resulting in significant losses. However, the classification model tends to incorrectly classify up- and down-regulation hours in neither direction instead of in the opposite direction (Figure 14). Thus, the combination of the binary variables and the mFRR price prediction model is satisfactory for the scope of this thesis.

Class	Precision	Recall	F1-Score
Down	0.74	0.79	0.76
Neither	0.63	0.61	0.62
Up	0.75	0.71	0.73

Table 1: Precision, recall, and F1-scores for the trained mFRR classification model in classifying the test data as down-regulation, up-regulation, or neither.

These price models are used in the data generation phase, while the capturable market volume restricts the decisions made in the SDDP model. However, in addition to the price models, the data generation phase requires information on another central source of uncertainty in the problem: the production-related uncertainty.

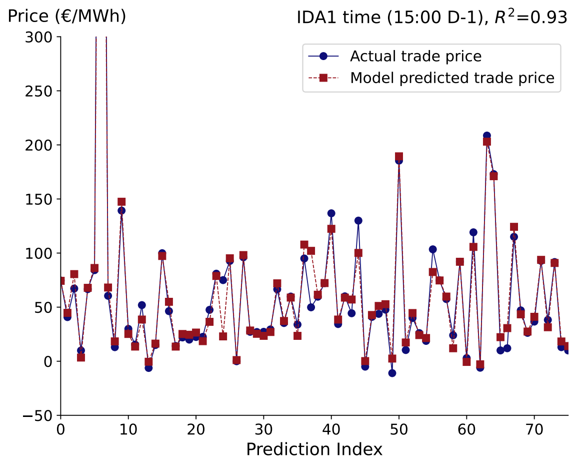

(a)

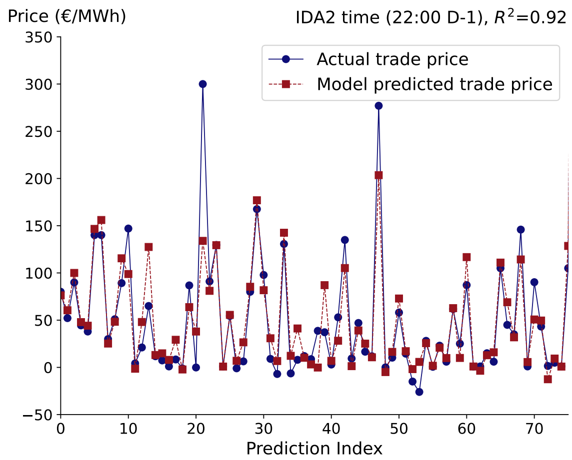

(b)

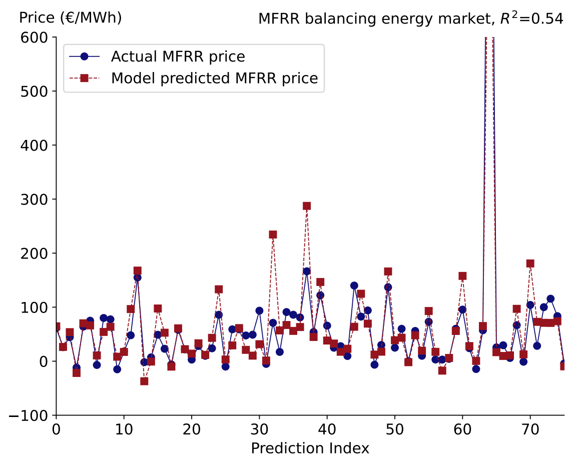

(c)

Figure 13: The first 75 values for the XGBoost model prediction and actual values in the test dataset for the IDA1 (a), ID2 (b) and mFRR (c) stages.

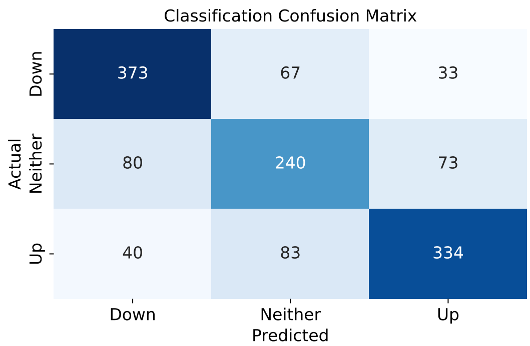

Figure 14: The confusion matrix displaying the model accuracy in predicting up- or downregulation.

4.3 Production Uncertainty

Renewable generation via wind and solar power is inherently unpredictable. At each decision point, the agent faces uncertainty regarding two renewable-related metrics: Finland's renewable generation in its entirety and the agent's own generation, which is correlated with the national renewable generation. The extent of the correlation between the agent's generation and the national total generation is pivotal, as it may allow the agent to act strategically in certain situations. We assume that the DA, IDA1 and IDA2 stages each have a forecasted generation value. In the mFRR node, which is only 15 minutes before generation, we assume that the forecast is perfectly accurate, i.e., the actual renewable generation.

Renewable generation forecasting errors are assumed to be randomly distributed. Furthermore, changes in forecasted generation between consecutive decision stages, for example between IDA1 and IDA2, are also assumed to be randomly distributed. Renewable generation uncertainty for the Finnish level is quantified using data obtained from Fingrid. Three different forecast datasets are assembled, representing forecasted generation for the entirety of day D at 12:00 D-1, 15:00 D-1 and 22:00 D-1. In general, forecasting errors are dependent on the time between the forecast and physical delivery. Thus, each hour has a different distribution the random change in forecast is sampled from.

Figure 15 represents the fitted distributions for the relative changes in forecasted generation at 12:00 for the periods between each decision: DA - IDA1, IDA1 - IDA2 and IDA2 - mFRR. As seen, the first two distributions are strongly centred around 0, i.e., the average change in forecasted generation between stages is relatively small. However, the final change in the forecast, i.e., the change from IDA2 to mFRR, clearly exhibits larger changes in forecasted generation. These phenomena are unsurprising, as the change in forecasted generation is highly dependent on the time between decision points [68]. The intervals between the first three stages are 3 and 7 hours, however the time interval from the IDA2 stage to physical delivery is 14 hours for the 12:00 case.

In the case of solar generation, the methodology is slightly different. Fingrid currently does not collect data in the same fashion for solar and wind, and thus forecasted generation at the IDA1, IDA2 and mFRR times are unavailable. However, ENTSOE collects data for the solar forecast at different time points, labelled "day-ahead", "intraday" and "current" [70]. Thus, we assign the "intraday" forecast to the IDA1 stage, and the "current" forecast to the IDA2 stage. Slight inaccuracies resulting from this assumption are not critical, as the effect of solar generation on price variation between stages is significantly smaller than the effect of wind [71]. Figure 16 represents the data and fitted distributions for the relative changes in forecasted Fingrid generation. As seen in the Figures, the general fit is relatively accurate. However, one notable difference to wind is the polarisation of changes in forecasted generation. In the case of solar, the forecasted generation can change from significant generation to exactly zero. Forecasting solar generation for days with partial cloud cover ahead of time can provide significant challenges, which could be one explanation for this phenomenon.

A different methodology is used for uncertainty regarding the agent's own gen-

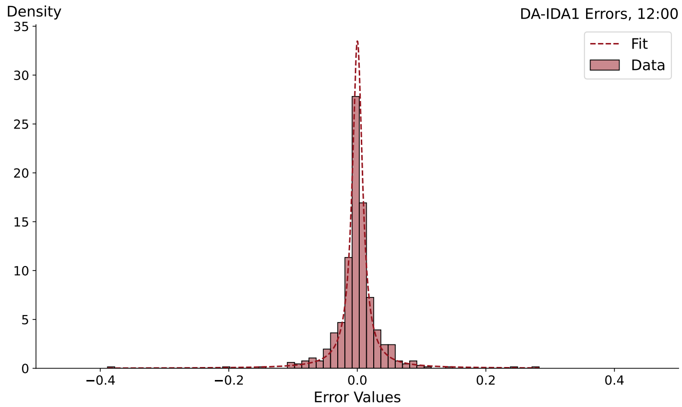

(a)

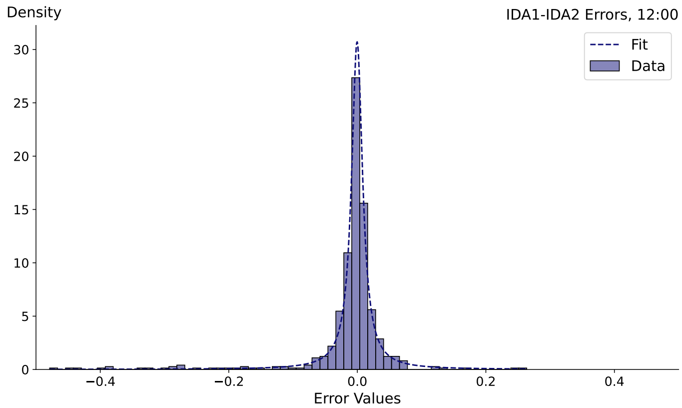

(b)

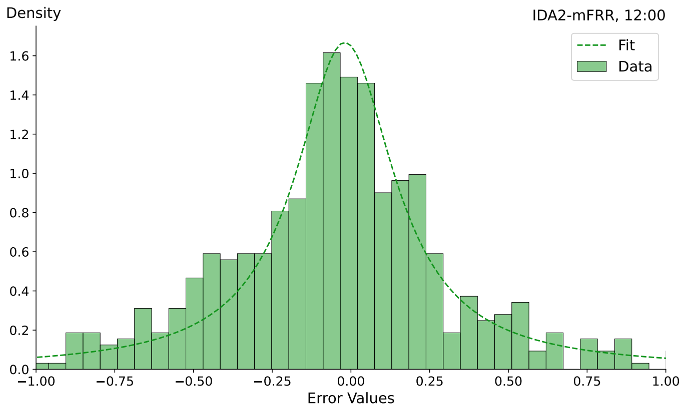

(c)

Figure 15: The data and fits for the relative changes in Fingrid's forecasted wind generation between nodes: DA-IDA1 (a), IDA1-IDA2 (b) and IDA2 - mFRR (c). The x-axis extent is [-0.5,0.5] in (a) and (b), and [-1, 1] in (c).

eration. Forecasting errors are once again assumed to be random for the agent's own generation. However, in this case, the important metric is the relation between

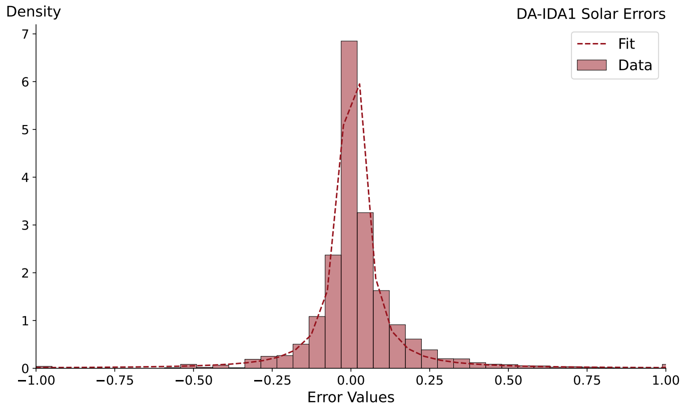

(a)

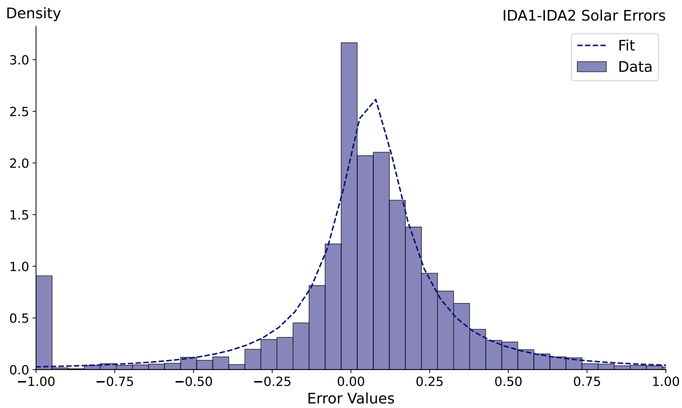

(b)

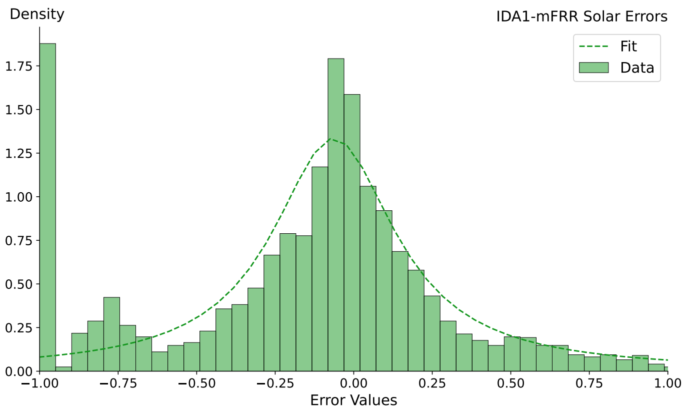

(c)

Figure 16: The data and fits for the relative changes in Fingrid's forecasted solar generation between nodes: DA-IDA1 (a), IDA1-IDA2 (b) and IDA2 - mFRR (c). The x-axis extent is [-1, 1] in all figures.

the national forecasting error $E_{National}$ compared to the error in own generation forecasting error, referred to as $E_{Singular}$. We assume that the relationship $\Re$ can be modelled by examining the percentage difference between forecast errors, i.e., $\Re = E_{Singular}/E_{National}$. To obtain the forecast data for these stages, we fit a distribution for the relative difference in errors between the agent's and Fingrid's day-ahead forecast. We can then simulate possible realisations of the agent's own generation forecast, while maintaining correlation with the large-scale forecast, with:

$$gf_{t+1} = gf_t(1 + D_{sample} \cdot E_{National}), \tag{2}$$

where D_{sample} represents a sampled value from the fitted distribution and gf_{t+1} is the generation forecast at stage $t + 1$. The best fitting commonly used distribution is the Cauchy distribution with parameters $\mu \approx 0.06$ and $\sigma \approx 0.60$ for wind park 1 (W1), and the Cauchy distribution with parameters $\mu \approx 0.07$ and $\sigma \approx 0.57$ for wind park 2 (W2).

For this thesis, data is available for two wind park day-ahead forecasts and actual wind generation for most of 2024. However, forecast data for the two intraday stages is unavailable. Thus, synthetic datasets are constructed by applying the same data relationship to each time period between decision points. Though this is not strictly realistic, the data does not affect any other part of the model — it can be replaced with actual data if it is available.

Figure 17 represents the data and fitted distributions for the two wind parks with available data $E_{Singular,1}/E_{National}$ and $E_{Singular,2}/E_{National}$. In the case of the agent's own solar generation, there is a lack of small-scale solar farm data. Thus, we use the third of the Swedish bidding areas (SE3) solar forecast and generation profiles for the day-ahead forecast and mFRR generation, because it is located at a similar longitude to Helsinki. For the stages in between, we assume that the agent's change in forecasted solar generation is related to the Fingrid solar generation according to the uniform distribution between -0.5 and 1.

4.4 Clustering and the Transition Matrix

At the current stage of the model workflow, 8000 (2000 x 4 stages) iterations of independent stochastic processes and the associated changes in price have been simulated. However, according to our preliminary experimentation, the proposed SDDP model requires a maximum of 100 - 300 nodes per stage to remain solvable within a reasonable time. Therefore, we aim to categorise the 8000 independent price iterations into 80 unique states, which capture different possibilities in price and generation realisations as accurately as possible. For this we use K-means clustering.

For the clustering phase, we combine the independent realisations for the IDA1, IDA2 and mFRR stages. Thus, the K-means algorithm is given a total of 8000 datapoints, which are to be grouped into 80 distinct clusters. We use the centroid of each cluster to represent a distinct state in the SDDP model. Each datapoint, and thus centroid, contains 6 different metrics: the market price, the forecasted generation for our agent (W1, W2 and S) and the forecasted national generation for wind and solar. The sizes of each cluster can vary significantly, as seen in Figure 18.

The final step of preprocessing before solving the resulting stochastic optimisation problem is calculating the transition matrix. This is relatively straightforward:

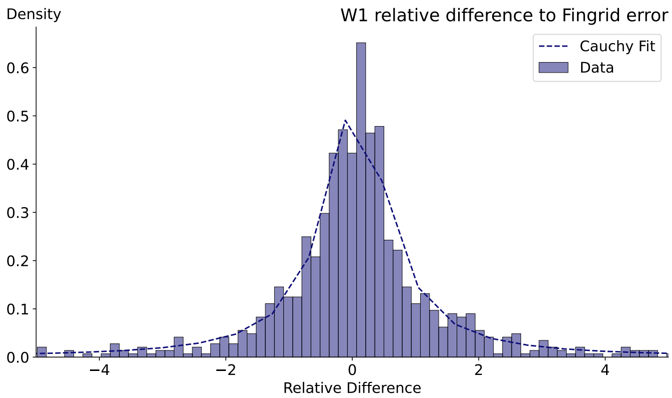

(a)

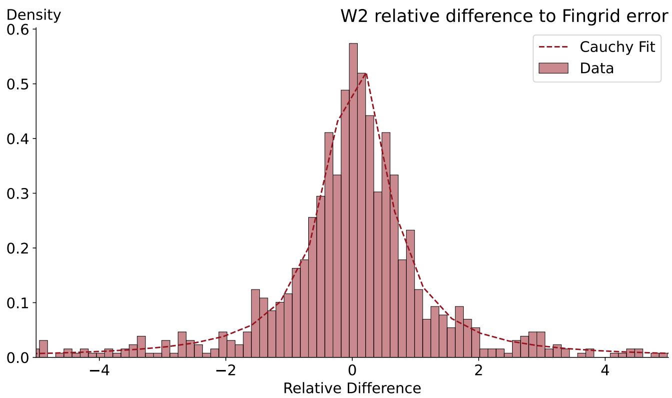

(b)

Figure 17: The data and fitted distributions describing the relative difference in forecasting errors for the agent's and Fingrid's generation forecasts.

beginning from the day ahead stage, 2000 stochastic independent realisations of the next market price and renewable generation are simulated. Each of the resulting realisations is then categorised using the same K-means grouping algorithm as above. The resulting transition probability to an arbitrary node can be calculated by dividing the amount of realisations grouped as belonging to that node by the total amount of simulations. This process is then repeated for every node of every stage.

4.5 SDDP Model Formulation

The primary goal of the agent is to generate the maximum amount of profit in all the considered markets, by choosing a set of control variables $\mathbb{U}$. The maximised function is thus the expected profit given a set of chosen control variables (Equation 1). The objective of the model is to return a policy dictating the amount of power bought and sold at each market stage, with each hour independent. The agent does not generate any offer curves in the SDDP model, instead, the only two control variables

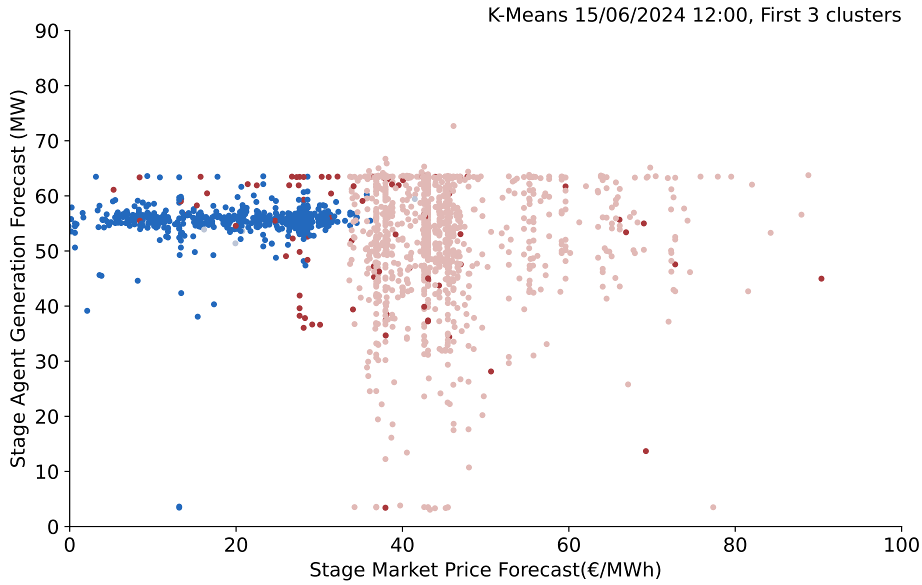

Figure 18: The price forecast and total agent generation of the clustered datapoints. Only the first three clusters are displayed.

for each of the four stages are the u_b and u_s variables, which represent the amount of power bought and sold in the market for each stage in MWh. In practice, the problem concerns the optimal allocation of available production. In this section, we present the mathematical formulation for the SDDP model.

The model has one state variable, which tracks the cumulative sum of bought and sold power. This variable is referred to with the term power balance (and denoted by Λ). The outgoing power balance value is mapped to the incoming value and the control variables by the function

$$\Lambda_i' = \Lambda_i + u_{b,i} - u_{s,i}, \ \forall i \in \{1, 2, 3, 4, 5\} \tag{3}$$

The power balance term can take both negative and positive values. It is linked to two imbalance variables, $\Delta^+ \geq 0$ and $\Delta^- \geq 0$, and another variable referred to as power $\mathcal{P}$. The imbalance variables represent the cumulative positive and negative imbalance, while power is the sum of these imbalances and the agents generation at that node:

$$\mathcal{P} = \Lambda_i' + G_{i,j} = \Delta_i^+ - \Delta_i^- + G_{i,j}, \ \forall i \in \{2, 3, 4, 5\}, \tag{4}$$

where $G_{i,j}$ represents the value of the generation at stage i and node j. Furthermore, as the imbalance can either be positive or negative at one point of time, we apply the constraints

$$\Delta_i^- \leq M_- \cdot (1 - \delta) \tag{5}$$

$$\Delta_i^+ \leq M_+ \cdot \delta, \tag{6}$$

where $\delta \in \{0, 1\}$ is a binary auxiliary variable and M_{-}, M_{+} represent upper bounds for the cumulative negative and positive imbalances. This constraint ensures that only one of the positive and negative imbalance terms are active at one stage.

The other state variable affecting the objective function is the electrolyser capacity, denoted by $0 \leq E \leq E_{maximum}$. $E_{maximum}$ represents the maximum electrolyser capacity, which we assume to be 60 MW in this model. The outgoing value for the electrolyser capacity is determined in the final stage by

$$E' = G_{i,j} + \Delta_i^+ - \Delta_i^-, \ \forall i \in \{5\}, j \in \mathbb{G}, \tag{7}$$

where $\mathbb{G}$ represents the set of possible generation scenarios for the agent.

The electrolyser can produce RFNBO-certified, low-carbon or fossil hydrogen. The RFNBO generation can be between 0 and the current electrolyser capacity:

$$0 \leq R \leq E' \tag{8}$$

The RFNBO component is determined from the electrolyser state value with

$$R = p_{i,j} + \alpha \cdot \Delta_i^+ + s, \ \forall i \in \{5\}, j \in \mathbb{G} \tag{9}$$

where α represents the RFNBO percentage of the bidding area in question and s represents a slack variable to relax the constraint in the case where the positive imbalance has a value higher than the maximum electrolyser capacity. For the sake of simplicity, we aggregate all non-RFNBO hydrogen to the same quantity. This hydrogen is referred to as non-RFNBO.

4.6 Day-ahead stage

Recall from Section 4.2.1 that the day-ahead stage is split into two separate nodes, allowing the node to be converted into a decision-hazard node, instead of a hazard-decision node. For this node, the stagewise objective is

$$u_{s,1}\rho_{DA,j} - u_{b,1}\rho_{DA,j}, \tag{10}$$

where ρ_{DA} is the forecasted day-ahead price. Furthermore, the control variables are constrained to discourage extreme deficits and surpluses compared to the scale of generation

$$0 \leq u_{s,1} \leq \Sigma_{z_1}^3 \gamma_z \tag{11}$$

$$0 \leq u_{b,1} \leq \Sigma_{z_1}^3 \gamma_z, \tag{12}$$

where the term $\Sigma_{z_1}^3 \gamma_z$ represents the sum of maximum generation capacities for the agent's own assets. These constraints ensure that the model policy remains at acceptable risk levels considering the agent's portfolio size.

The agent does not observe the realisations of the price uncertainty until the next node. Decisions made for this stage must equal the previous node's controls. In this node, the stage objective is

$$u_{s,2}\psi_{DA} - u_{b,2}\psi_{DA}, \tag{13}$$

where ψ_{DA} represents the randomly distributed residual for the day-ahead price prediction. Furthermore the control variables $u_{s,2}$ and $u_{b,2}$ are constrained to be equal to the controls in the previous stage:

$$u_{s,1} = u_{s,2},\ u_{b,1} = u_{b,2}. \tag{14}$$

4.6.1 Intraday stages

Similarly to the day-ahead stage, in the IDA1 and IDA2 stages (nodes 3 and 4), the stage objective is

$$u_{s,i}\rho_{j,IDA_k} - u_{b,i}\rho_{j,IDA_k},\ i \in \{3,4\},\ j \in \mathbb{S},\ k \in \{1,2\}, \tag{15}$$

where $u_{s,i}$ and $u_{b,i}$ represent the amount of power bought or sold at stage i, ρ_{j,IDA_k} represents the forecasted intraday price for IDA stage k and scenario j and $\mathbb{S}$ represents the set of possible price scenarios.

Furthermore, in both stages, the controls are constrained to be less than the randomly distributed volume:

$$0 \leq \mathbb{U}_i \leq \varepsilon_{IDA_k},\ i \in \{3,4\}, k \in \{1,2\}, \tag{16}$$

where ε_{IDA_j} represents the randomly distributed market volume parameter. This market volume represents the maximum traded power for that stage while assuming that the agent is in a price-taker position. This constraint is not exactly realistic, as in a real situation bidding can not be determined by an assumed capturable market volume. However, a constraint such as this is needed in the validation of the model, which is done based on historical data on the market volume. To ensure that the generated revenue is realistic considering the actual market characteristics, the volume constraint is applied.

4.6.2 mFRR stage

The mFRR stage is different in nature to earlier stages. Power can still be traded, however, each hour is either up-regulating, down-regulating or neither. In the case of up-regulating, power can only be sold, whereas in a down-regulating market, power can only be bought. Furthermore, the final mFRR stage is where the effect of the cumulative power balance is observed. Additionally, the hourly RFNBO and non-RFNBO generation for the electrolyser is determined. Furthermore, the objective function contains two penalty terms, which discourage the accumulation of significant negative imbalances of power. Thus, the objective function for the mFRR stage is of the form

$$\begin{aligned} u_{s,5} \cdot \rho_{j,5} \cdot r_j^+ - u_{b,5} \cdot \rho_{j,5} \cdot r_j^- + R \cdot mp_{RFNBO} + (E' - R) \cdot mp_{N-RFNBO} \\ - c_1 \cdot \Delta_5^- \cdot \lambda - \Delta_5^- \cdot u_{s,5} \cdot \rho_{j,5} + c_2 \cdot \mu_{Surplus}, \end{aligned} \tag{17}$$

where r_j^+ and r_j^- are binary indicator variables, representing if the hour is up-regulating or down-regulating (or neither) and c_1 and c_2 are constant terms. The variables mp_{RFNBO} and $mp_{N-RFNBO}$ represent the non-electricity marginal profit excluding power for RFNBO hydrogen and the non-electricity weighted-average marginal profit for low-carbon and fossil hydrogen. The two final terms are the penalty terms: the term including λ is a general term for penalising excessive deficits in normal operation. The second term is only active when the hour is up-regulating. This strongly discourages deficits when the final hour in question may be up-regulating, as this can coincide with significant losses in revenue. Furthermore, $\mu_{Surplus}$ is a term only active in situations where the day-ahead price is negative. In this case, it penalises a surplus according to

$$\mu_{Surplus} = \rho_{j,5} \cdot \Delta_5^+. \tag{18}$$

Similarly to the intraday stages, the control variables for traded volume are constrained by a random market volume term. This is done to ensure that the bought and sold volumes are within acceptable and realistic values., i.e.,

$$0 \leq \mathbb{U}_5 \leq \varepsilon_{mFRR}. \tag{19}$$

4.7 Collecting the Optimal Policy

The SDDP model returns an optimal policy for the agent, given a certain incoming state, which governs the amount of power bought and sold for each stage. However, these policies are determined based on the value of the predicted market price at that stage, while the realisation of that price is not observed within the model. Thus, purely relying on the outputs of the base SDDP model could potentially lead to situations where the agent buys or sells power irrelevant to the realised price, which could turn out to be significantly smaller or larger than the prediction. Thus, to account for this we construct a decision tree structure, which enables us to incorporate price offer thresholds into the optimal policy.

The optimal control in a certain stage depends on three components: the realised scenario, i.e., the node, the incoming state and the noise realisation. Regardless of the state of the agent in our market, the noise realisation and the node, or the scenario observed, are the same for that stage. Thus, as the only state variable affecting model decisions is the cumulative sum of bought and sold power, i.e., the power balance state variable, we can construct the binary tree presented in Figure 19. Each node has two children, representing the situations where either the offer is declined or accepted. In the case where the offer is accepted, the outgoing state is updated with the offered volume by the policy. Otherwise, the outgoing power balance remains the same. The power balance at any given node is thus just the cumulative sum of its parent nodes with accepted offers.

This structure allows the agent to determine price thresholds for each stage by assigning an upper bound in the case of buying power, and a lower bound in the case of selling power. This is applied to the DA, IDA1 and IDA2 stages. The allowed percentage change is inversely proportional to the magnitude of the predicted price. We perform sensitivity analysis for this in the next section. In the validation of the policy, we disregard the optimal model policy of the final stage because of market regulation. Instead, we assume that the agent must offer all available regulation capacity to the market at the encountered marginal cost.

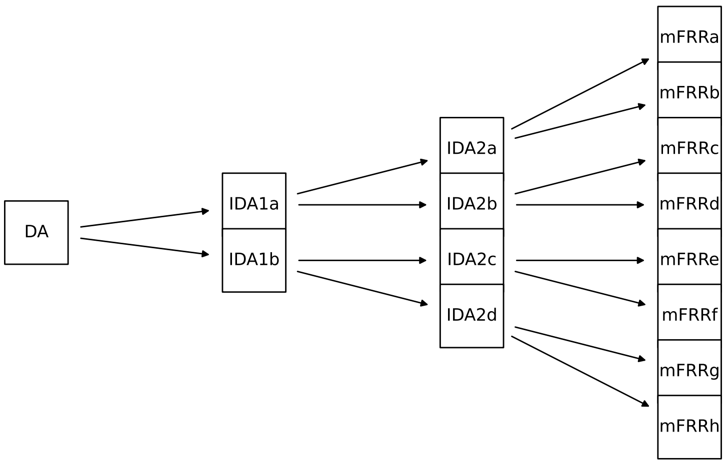

Figure 19: The decision tree structure representing the possible obtained policies depending on offer success or failure.

5 Results

In previous sections, we have presented the methodology for constructing a model for the optimisation of trading with a VPP in multiple electricity markets at discrete time points. In this section, we present the results from the model. We first present a visualisation of the policy for a single hour. This policy represents the output of the first stage of the model, which only determines the buy and sell volumes for each stage. Then, to assess the suitability of our model, we compare the generated profits of the model from January to June 2024 to a baseline strategy. Of the examined period, 24 hours were excluded because of data issues. These include the entirety of the 27^{th} of June, and 23 hours across the rest of the time interval. Thus, the final length of the time interval is 4292 hours.

5.1 Model output for a single hour

The output of a single model iteration is a policy, determining the optimal decision given an incoming state and a noise realisation. The first stage decision is made based on the forecasted price and generation levels. However, subsequent decisions not only depend on the random noise realisation representing available market volume but also on the decisions and random realisations of previous stages and the incoming state.

The output of a single SDDP solution for January 1^{st} 01:00 is displayed in the Figures 20 and 21. Figure 20 represents the power bought and sold in each stage, As stated before, the first and second-stage decisions, representing the day-ahead nodes, only contain one possible decision. However, the decisions afterwards can contain significant deviations depending on the incoming state and realisation of the random noise variable. Each Figure contains a solid line, representing the median decision. The shaded areas represent the 0-100, 10-90 and 29-75 percentiles. As seen in the Figure, both the buy and sell control variables can differ significantly, ranging from 0 to 120 MW.

For this hour, the agent in question sells a large portion of available forecasted power in the day-ahead market. In the first intraday auction stage, the median decision involves selling a small amount of power. However, in some of the realisations, the optimal decision is for the agent to buy generation, whereas in other scenarios the optimal is to sell power. In the second intraday stage, the median decision is to buy approximately 5 MW of power. However, in some scenarios, the agent sells significant amounts of generation, nearing 80 MW.

The eventual available power is a function of the cumulative sum of applied control variables for each stage and the generation at each possible node. This can differ significantly, as seen in Figure 21, which displays the total power available and the power balance parameter. We see that the median available power at the final stage is between 40 and 50 MW. However, in some scenarios, the power available is at a deficit of a similar magnitude. Furthermore, the largest surplus scenarios reach approximately 70 MW. These surpluses may occur in situations where the second intraday auction stage has a very low price, resulting in the agent buying a significant amount of generation based on the opportunity for significant profit in certain scenarios

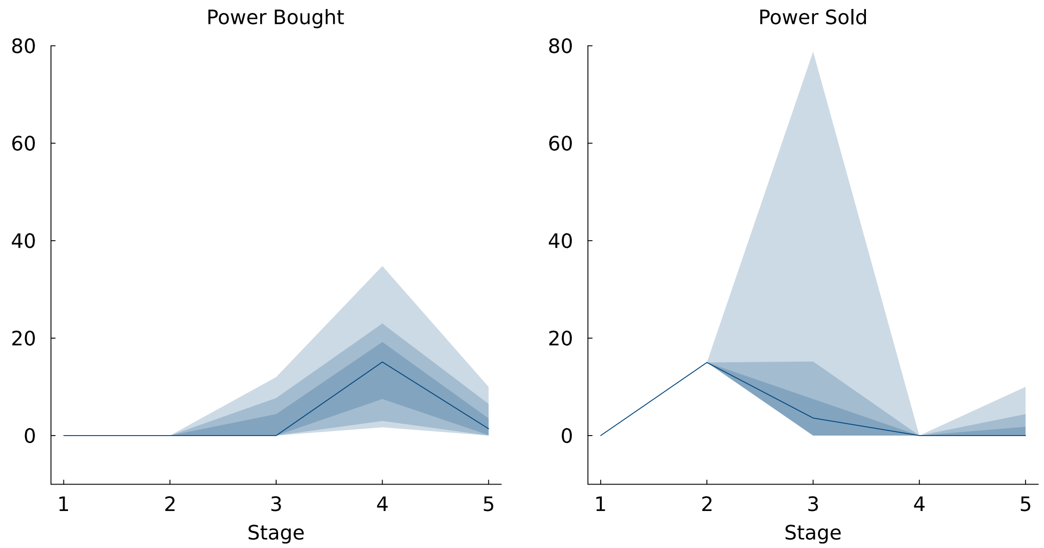

Figure 20: A plot of 300 simulations for the control variable decisions for buy and sell across each stage.

in the mFRR market.

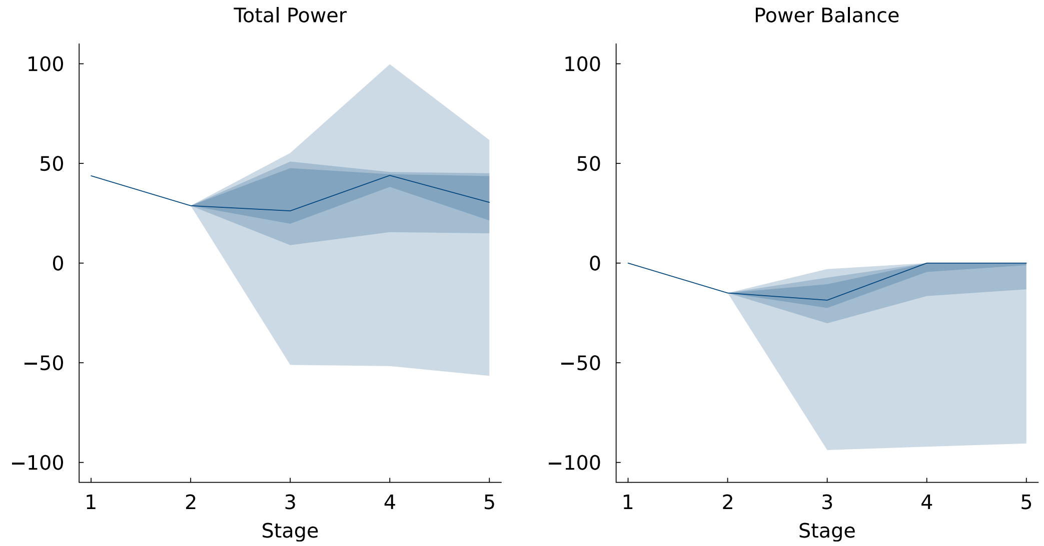

Figure 21: The corresponding 300 scenarios for total available power and power balance at each stage, dependent on the control variables buy and sell.

5.2 Comparison with the baseline strategy

Each optimal policy for an hour in the examined period returns buy and sell decisions given an input state. We then derive a scenario tree of all the potential decisions, given a price threshold determining if the offer is accepted or declined (such as in Figure 19). Applying this decision tree to each stage of each hour, we can determine the generated revenue over the entire period. This generated revenue is then compared to a naive strategy.

The time period for the comparison overlaps with the training data for the price models. However, this should not affect results much, as the price models are given features based on randomly sampled values for wind forecasting errors. Furthermore, as the 80 states are the same across all stages, the effect of the overlap between the training data and this comparison on the result should be low. However, it should be kept in mind when examining results. Additionally, the data used to examine profits generated is not the actual intraday action data, instead is based on the continuous intraday market trading data. This is discussed in the final paragraph of Section 2.1.2.

The naive strategy involves a different agent, possessing the same information regarding forecasted generation. In the naive strategy, the agent prioritises the electrolyser capacity. If the market price is below the non-electricity marginal profit of producing RNFBO and non-RFNBO hydrogen, the agent purchases power until the electrolyser is at full capacity. All residual forecasted generation is offered to the day-ahead market at any price. In the case of the price being higher than the marginal profit of RFNBO hydrogen, the agent offers all of its forecasted generation to the market. For later stages, the agent operates in a similar fashion, however, decisions are restricted by the same market volume parameter as in the SDDP case. In the event of imbalances stemming from forecasting errors, the agent purchases or sells power to keep the net difference of power between the current stage and the day-ahead stage as low as possible. Additionally, when the price at any stage increases over the marginal profit of RFNBO-produced hydrogen, the agent sells as much generation as possible. If the electricity price exceeds the marginal profit of non-RFNBO hydrogen, the agent sells as much grid-sourced electricity as possible, while keeping the RFNBO-certified power from its own assets. In the mFRR stage, the agent offers all available capacity at marginal cost for both up-regulation and down-regulation. In the case of a surplus of generation and all available market volume sold as down-regulation, the residual is curtailed if possible.

In the case of the optimal policy, all decisions in the day-ahead and intraday stages are made based on the SDDP model outputs. However, in the final stage, the logic for operation is the same as in the case of the naive strategy. If the electricity price exceeds the marginal profit of non-RFNBO hydrogen, the agent sells as much grid-sourced electricity as possible, while keeping the RFNBO-certified power from its own assets. In the mFRR stage, the agent offers all available capacity at marginal cost for both up-regulation and down-regulation. In the case of a surplus of generation and all available market volume sold as down-regulation, the residual is curtailed if possible. This similarity between the two strategies stems from the fact that the situation in the mFRR market involves only one market without any subsequent opportunity costs.

Thus according to the market regulation in Section 2, both agents must offer generation at their encountered marginal cost.

5.2.1 Profit Generated by Each Strategy

The agent making decisions according to the optimal SDDP strategy, combined with the price thresholds thresholds, generates a profit of 14.13 M€ in the first half of 2024. This is a relative increase of approximately 4.18% compared to the naive strategy, which generated approximately 13.54 M€ in the same period. The profit generated from each market and hydrogen sales for both strategies are displayed in Table 2. As seen in the table, the optimal and baseline strategies differ significantly in where profit is generated. The agent operating with the optimal strategy generates significantly more profit in the day-ahead market than with the baseline strategy. Furthermore, the net results from other power market stages are larger, with both IDA stages seeing significantly more activity. The baseline strategy generates more profit from RFNBO, especially from Non-RFNBO hydrogen sales.

(M€)	DA	IDA1	IDA2	mFRR	RFNBO	N-RFNBO	Imbalance
Optimal	2.52	0.23	-0.11	0.81	10.22	0.85	-0.43
Base	-3.88	0.07	-0.03	0.43	11.64	7.78	-0.40

Table 2: Net profit generated from each individual source for the optimal and baseline strategies. The numbers are rounded to two decimal places with the unit (M€).

On average, the optimal strategy is a net seller in the day-ahead market by -3.9 MW. This is the opposite behaviour to the baseline strategy, which purchases a total of 26.7 MW from the day-ahead market on average (Figure 22). To cover for the overbuying, the optimal strategy is a net purchaser in the IDA2 and mFRR markets. Slightly counterintuitively, the optimal strategy has a positive imbalance on average, whereas the baseline has a negative imbalance. This discrepancy is due to a small number of hours where the optimal model overbuys in the day-ahead market at considerably cheaper prices, with the intention of potentially profiting at a later stage. However, when the residual power is unable to be offloaded, the agent ends up with a positive imbalance. In general, these hours occur simultaneously with a large amount of the agent's own generation, resulting in the residual available power showing up in the imbalance, instead of the electrolyser generation. The baseline strategy produces more hydrogen by over 20 MW compared to the optimal strategy.

Further differences in trading behaviour between the two strategies are evident when examining the volume-weighted average prices (VWAP) for purchased and sold power (Figure 23). In general, the optimal strategy has a significantly lower purchase price compared to the baseline strategy, especially in the day-ahead market and the first intraday auction. Here, the volume-weighted average purchase price is more than 40 €/MWh higher for the baseline strategy. This phenomenon is less significant in later markets, however it is still clearly present.

On the other hand, the baseline strategy has much higher volume-weighted average prices when examining sold power in each market. The largest difference is in the first

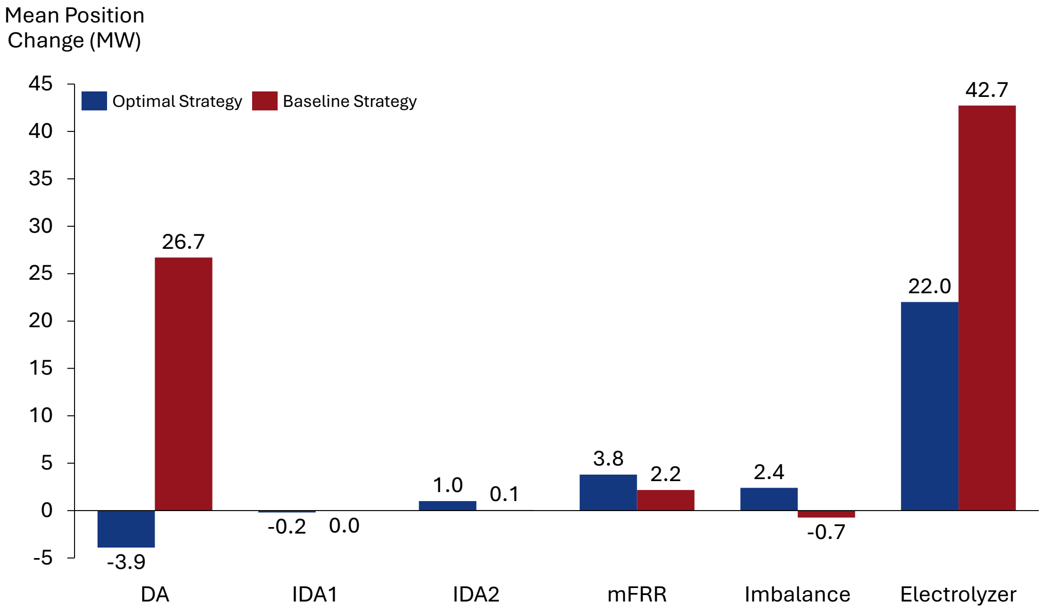

Figure 22: The average change in position, i.e., average sale, generation or purchase, for each profit generating source. The electrolyser contains both RFNBO and Non-RFNBO hydrogen.

and second intraday auctions, where the captured sale price is more than double for the baseline strategy compared to the optimal strategy. The smallest difference between the two strategies is in the mFRR stage, however, even here the baseline strategy has a significantly higher volume-weighted average sale price.

Though the significantly higher VWAP for the baseline strategy may seem opposite to the expected behaviour, the situation becomes clearer when examining the total traded volumes in each market across the entire period (Table 3). The optimal strategy has a day-ahead total volume amounting to less than 50% of the traded power in the baseline strategy. However, the optimal strategy trades approximately 30 times more power in the IDA1 stage and 15 times more in the IDA2 stage compared to the baseline strategy. Additionally, the mFRR trade volume is nearly twice as large in the optimal strategy.

Strategy	DA	IDA1	IDA2	mFRR
Optimal	55900 MW	8900 MW	14600 MW	23200 MW
Baseline	127700 MW	300 MW	1000 MW	12700 MW

Table 3: The sum of all traded volumes rounded to the closest hundred in all four market stages for both strategies.

Thus, combining the information of Figure 23 and Table 3, the optimal strategy is significantly more active in finding profitable trading situations. However, the baseline strategy only modifies its position in the market when the situation is profitable, i.e., when the price is above the non-electricity marginal profit of hydrogen. Thus, the

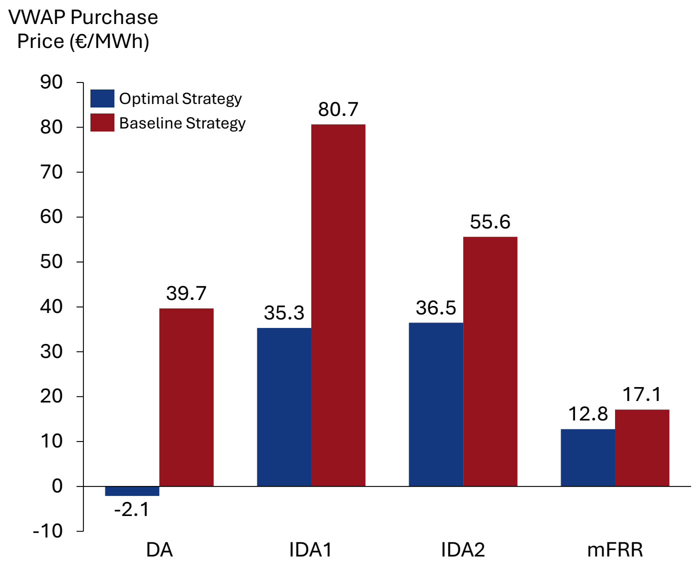

(a)

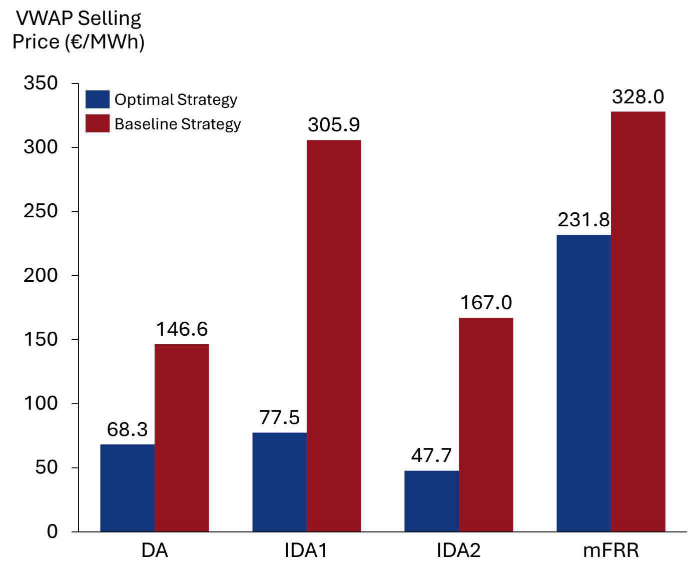

(b)

Figure 23: The volume-weighted average prices (VWAP) for the optimal and baseline strategies in all four market stages.

VWAP for sold power is significantly higher, because the value only captures the highest price peaks. The optimal strategy may have a smaller VWAP for sold power in each market, but the model is able to find more profitable positions more often.

The optimal policy generates more profit in the power market, using the electrolyser as a backup in situations where the surplus or deficit of generation can not be covered. This can be seen in the average hourly profit generated from each source (Figure 24). The optimal policy on average generates 2.2 k€ more profit from the DA, IDA1, IDA2 and mFRR stages. On the other hand, the profit generated from RFNBO and non-RFNBO hydrogen is higher for the baseline policy, especially in the case of non-RFNBO hydrogen. However, the optimal strategy is able to capture nearly the same amount of profit from RFNBO hydrogen sales.

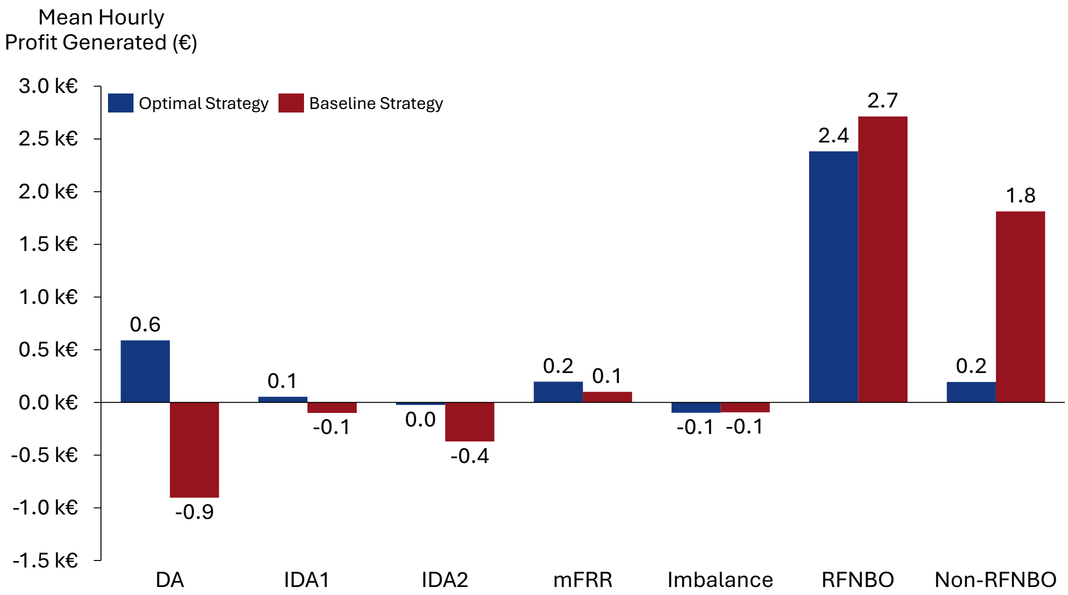

Figure 24: The average hourly profit for all profit sources for the optimal and baseline strategy.

In addition to the metrics above, another key difference between the two strategies is related to the variety of offered volumes in different markets. The optimal strategy has a wider distribution of traded volumes in all markets, most notably in the day-ahead market and the second intraday auction stage. On the other hand, the baseline strategy is more conservative in its trades, with a much narrower distribution of trade volumes in all markets. Furthermore, the optimal strategy has significantly more outliers. These characteristics reinforce the suggestion of the optimal strategy being more aggressive in trades, while the baseline strategy is more conservative.

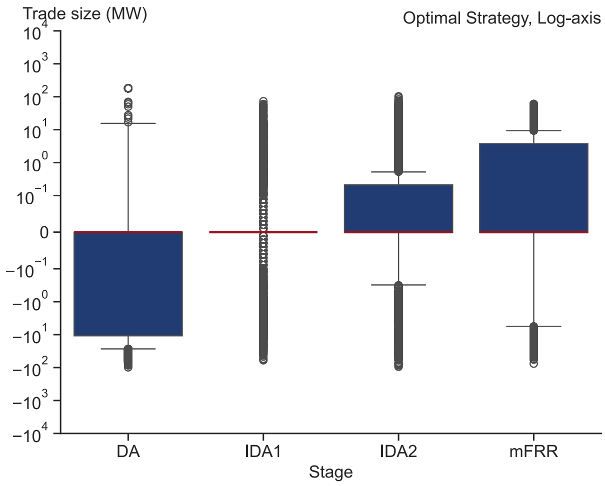

(a)

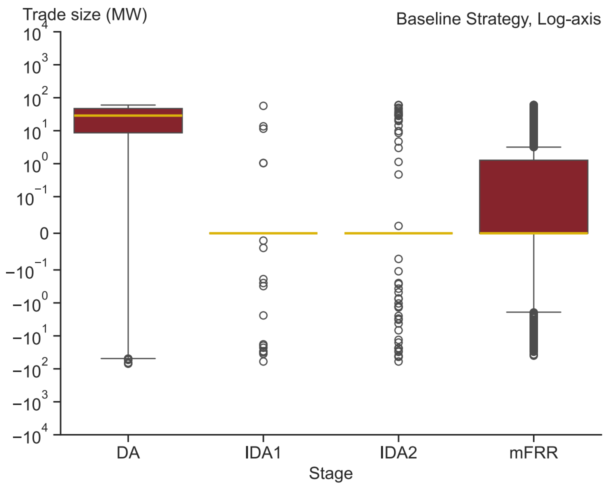

(b)

Figure 25: Boxplots representing the distribution of trade volumes across the entire time period for the optimal (a) and baseline (b) strategies. The red lines (a) and black lines (b) represent the median, the box the 25 - 75 percentiles and the whiskers the 0 and 100 percentiles, excluding outliers. The axis is logarithmic in both (a) and (b).

6 Discussion

The experimental results indicate that a stochastic dual dynamic programming (SDDP) model can increase the generated profit for a VPP consisting of variable renewable generation, operating under price and generation uncertainty. The increase in profit for the first half of 2024 was approximately 4.18%. The main driver of the increased profit was the more aggressive behaviour in the market stages, especially in the first and second intraday auctions. Furthermore, typical behaviour in the day-ahead market was different between the two strategies, with the optimal strategy being a net seller on average, while the baseline strategy was a net buyer. In the case of the optimal strategy, a key phenomenon potentially increasing the profit compared to the baseline strategy was the aggressive and speculative overselling or overbuying of generation in earlier markets. In these situations, the model typically anticipates a scenario, where it can rebuy or sell power at a low cost. Though these situations may not always generate a profit, when it does the profits can be significant.

The stages used in this model were the day-ahead market, the first two intraday auctions and the mFRR balancing energy market. These markets were used as decision points because they provided discrete time points, and trading power was available for all hours. Notably, IDA3 was left out of the problem for simplification, due to power trading only being allowed for hours after 12:00 D. However, this introduced a phenomenon where the intraday auctions were close in time to each other (15:00 and 22:00). However, the mFRR stage for the evening hours could be up to 23 hours after the second intraday auction. Thus, including the third intraday auction, or some other discrete time point could introduce more possibilities for the trading strategy, and potentially improve model performance.

The model has some notable areas of improvement. One clear area concerns the unrealistic assumptions regarding the capturable market liquidity. In an actual setting, the offered amounts are not restricted, and instead, the agent must consider the effects of their own offered generation on the realised price. This is especially relevant in settings such as intraday auctions, which have not seen very high trading volumes since their establishment. However, one possible solution for an agent using this model in practice is always offering all their generation in the model forecasted price (or a similar price level). In this case, the offered volume is either fully or partially activated, or not at all. However, this is most likely ineffective in the case of trying to find optimal allocations of power. The use of an external market volume prediction model in combination with the SDDP model of this thesis is another option. The trading volumes in the continuous intraday market will likely be highly correlated with volumes at each auction point. Thus, creating an accurate model for predicting market volume realisations and their probabilities may be possible.

Another area for potential improvement is the accurate penalisation of situations where the model has a deficit or surplus of power. In this thesis, deficits were penalised by subtracting the deficit multiplied by the up-regulating price from the objective function at the final stage. However, as the imbalance settlement is settled by the maximum of the volume-weighted average price in the aFRR market and the hourly mFRR price, the model does not adjust for the aFRR effect. In this thesis, to account for the effect of the aFRR market on prices, another penalty factor was subtracted from the objective function to further disincentivise deficits. However, including a realistic heuristic for the effect of the aFRR price on the imbalance settlement would be a key area for improvement.

The model faces some other shortcomings in addition to the market volume issue. SDDP is generally suitable for the modelling and optimisation of linear problems with stochastic elements. However, the power market exhibits nonlinear behaviour in multiple situations, which presents challenges for SDDP. The solution in this thesis was to simulate independent stochastic realisations for the nonlinear elements of the problem. This however presented its own problems, mainly concerning the dimension of information given as input to the SDDP model. In the case of this model, each state had six different data points. The amount of states is restricted to be 80 due to computational constraints. Thus, as the amount of states is relatively small, the differences between different scenarios could be significant, and potentially none can be suitable representatives for that actual realised state. Thus, the reality of the actual situation faced by the agent could be lost in the data generation phase of the model, even though the SDDP model itself could converge to an optimal solution.

In general, employing more sophisticated methods for the data generation would most likely improve model performance. The accuracy of price models, especially in the mFRR stage could potentially be significantly improved by including additional data and new predictors. Additionally, the training datasets are regrettably small. Furthermore, energy markets tend to exhibit black swan events from time to time, i.e., significant outlier periods, especially in markets after the day-ahead market. Combined with a small dataset, this results in significant challenges for predicting the most severe outlier events. Though the chosen models perform at a satisfactory level from the perspective of this thesis, in practice the accuracy of these models is integral in profit generation.

Furthermore, the methodology for creating possible scenarios for a single hour — by first simulating the stochastic elements of the problem and then categorising using a clustering algorithm — could also be refined. For example, applying importance weights for the most important metrics, price and the agent's generation, could be a possible solution for ensuring that these metrics cover the possible sample space at regular enough intervals.

However, SDDP may not simply be entirely suitable for a problem involving both generation and price uncertainty, which are both correlated with each other. Other models, involving neural networks or reinforcement learning applications may outperform the model presented in this thesis. Furthermore, the Nordic power market will transition to a 15-minute time interval, instead of an hour-long time interval in 2025 [72]. This will increase the number of hours requiring a solution from 24 to 96, increasing computation time significantly. Though parallelising this process is relatively simple, this still may not be computationally tractable for a trader, who would most likely want to make decisions rapidly.

Finally, the experimental results of this thesis may not reflect actual obtainable profits. The used electrolyser is assumed to be a perfect source of demand, meaning that increases or decreases in generation are independent of decisions in other hours.

Furthermore, no costs are associated with shutdowns, and no minimum or maximum capacity constraints are applied. Furthermore, the profits gained in intraday auctions may not prove to be as large, as the model does not use actual auction data. Instead, the data used is aggregated from the continuous intraday market for the time periods between each auction time point. This modelling decision was made due to intraday auctions being a new phenomenon in Finnish energy markets. Traded volumes are low — the median trade volume is 0 MW — though constantly increasing. Thus, the market price is nearly always coupled in the entire Nordic region. The challenge in low trading volumes and a coupled Nordic price from the perspective of this thesis is that the relationship between local forecasting errors in Finland and intraday auctions becomes muddled, with forecasting errors in other Nordic bidding zones, or other factors, becoming dominant drivers of prices. However, a central assumption for this modelling choice is that traded volumes in intraday auctions are to increase in the future, resulting in more frequent decoupling of Nordic bidding zones in intraday auctions. This would strengthen the correlation between local forecasting errors and intraday auction prices becoming more evident, making the model of this thesis nearly directly applicable to actual intraday auctions.

7 Conclusion

This thesis developed a model for optimising the trading behaviour of a wind, solar and renewable hydrogen portfolio. The agent operated in the day-ahead, intraday auctions 1 and 2 and the mFRR balancing energy market. The thesis first presented a methodology for generating a transition matrix and 80 scenarios via simulation of a stochastic process. These were then used by a stochastic dual dynamic programming (SDDP) model to solve the amount of traded volume in each market stage, To include simple price thresholds in these offers, a binary tree representing the state of the agent in the case of an offer being accepted or rejected was collected.

The improvement for the SDDP-derived solution was 4.18% for the first half of 2024 when compared to a baseline strategy, representing the strategy of an agent trading power according to a predefined heuristic. The baseline strategy was not a poor strategy, however it did not allow for any strategic overbuying or -selling, instead emulating the operation logic of an agent with a reasonable power market understanding. The main drivers of the increased profit for the optimal policy were the aggressive overbuying and -selling in profitable situations, the higher trading volumes in all three markets and the more monetarily efficient allocation of power in the market stages. The optimal strategy produced a significantly lower amount of Non-RFNBO hydrogen, instead using this capacity as a hedge to allow speculative trading in earlier market stages.

The limitations identified in this model concerned the generation of accurate and realistic scenarios, the computational efficiency and the constraints for traded volumes representing the random market volume assumptions. A direction for further research would involve the fine-tuning of the scenario generation and price prediction models. Furthermore, evaluating the potential for the inclusion of two external models — representing offer thresholds and a market volume prediction — to be used in combination with the SDDP model is another area for further research,

However, all models make assumptions and simplifications regarding the trading of a market operator. The assumptions made in this model are moderately realistic, and the model could certainly be used in assistance of an agent operating a VPP. As shown in this thesis, strategic bidding can generate excess profits compared to a more naive strategy. The improved profits would not only increase the buildout of renewable projects but also increase system efficiency by allocating power based on market signals.

References

[1] *ENTSO-E Transparency Platform*. https://transparency.entsoe.eu/. 2024.

[2] Fingrid. *Wind Power Generation*. https://www.fingrid.fi/en/electricity-market-information/wind-power-generation/. Accessed: 2024-07-19.

[3] Fingrid. *Solar Power*. https://www.fingrid.fi/en/electricity-market-information/solar-power/. Accessed: 2024-07-19.

[4] Guanghao Wang et al. "The Impact of Renewable Energy on Extreme Volatility in Wholesale Electricity Prices: Evidence from Organisation for Economic Co-operation and Development Countries". In: *Journal of Cleaner Production* (2024), p. 144343. ISSN: 0959-6526. DOI: https://doi.org/10.1016/j.jclepro.2024.144343. URL: https://www.sciencedirect.com/science/article/pii/S0959652624037922.

[5] Linh Phuong Catherine Do, Štefan Lyócsa, and Peter Molnár. "Residual electricity demand: An empirical investigation". In: *Applied Energy* 283 (2021), p. 116298. ISSN: 0306-2619. DOI: https://doi.org/10.1016/j.apenergy.2020.116298. URL: https://www.sciencedirect.com/science/article/pii/S0306261920316846.

[6] Wood Mackenzie. *Energy Transition: Investing in a High-Interest Rate Era*. 2024. URL: https://www.woodmac.com/horizons/energy-transition-investing-in-a-high-interest-rate-era (visited on 12/03/2024).

[7] Productivity Commission. *Electricity Network Regulatory Frameworks: Appendix C*. Report by the Australian Government. 2013. URL: https://www.pc.gov.au/inquiries/completed/electricity/report/28-electricity-appendixc.pdf (visited on 10/03/2024).

[8] Abolfazl Khodadadi et al. "Nordic Balancing Markets: Overview of Market Rules". In: *2020 17th International Conference on the European Energy Market (EEM)*. 2020, pp. 1–6. DOI: 10.1109/EEM49802.2020.9221992.

[9] Nord Pool Group. *Nord Pool Reports Robust Trading Figures for 2023*. https://www.nordpoolgroup.com/en/message-center-container/newsroom/exchange-message-list/2024/q1/nord-pool-reports-robust-trading-figures-for-2023/. Accessed: 2024-10-03. 2024.

[10] ENTSO-E. *Single Day-ahead Coupling (SDAC)*. https://www.entsoe.eu/network_codes/cacm/implementation/sdac/. Accessed: 2024-10-03. 2024.

[11] National Energy System Operator (NESO). *How is Electricity Priced?* https://www.neso.energy/energy-101/electricity-explained/how-electricity-priced. Accessed: 2024-10-03. 2024.

[12] Agency for the Cooperation of Energy Regulators. *Revised REMIT: ACER clarifies new obligations for non-EU market participants and persons professionally arranging or executing transactions*. https://www.acer.europa.eu/news-and-events/news/revised-remit-acer-clarifies-new-obligations-non-eu-market-participants-and-persons-professionally-arranging-or-executing-transactions. Accessed: 2024-10-02. 2024.

[13] Nick Hubble. *The Marginal Analysis That Undermines Wind and Solar Power*. https://daily.fattail.com.au/the-marginal-analysis-that-undermines-wind-and-solar-power/20230729/. Accessed: 2024-10-03. 2023.

[14] Richard Green. "Electricity and markets". In: *Oxford Review of Economic Policy* 21.1 (2005), pp. 67–87.

[15] Frank Sensfuß, Mario Ragwitz, and Massimo Genoese. "The merit-order effect: A detailed analysis of the price effect of renewable electricity generation on spot market prices in Germany". In: *Energy policy* 36.8 (2008), pp. 3086–3094.

[16] Nord Pool Group. *Euphemia Public Description*. https://www.nordpoolgroup.com/globalassets/download-center/single-day-ahead-coupling/euphemia-public-description.pdf. Accessed: 2024-10-03. 2020.

[17] Fingrid. *Congestion Income*. https://www.fingrid.fi/en/electricity-market-information/congestion-income/. Accessed: 2024-10-03. 2024.

[18] Nord Pool Group. *Intraday Trading*. https://www.nordpoolgroup.com/en/trading/intraday-trading/. Accessed: 2024-10-03. 2024.

[19] Next Kraftwerke. *Intraday Trading: Definition, Theory, and Practice*. https://www.next-kraftwerke.com/knowledge/intraday-trading. Accessed: 2024-10-03. 2024.

[20] NEMO Committee. *Information Package About Intraday Auction*. https://www.nemo-committee.eu/assets/files/information-package-about-intraday-auction.pdf. Accessed: 2024-10-03. 2021.

[21] Richard Scharff and Mikael Amelin. "Trading behaviour on the continuous intraday market Elbas". In: *Energy Policy* 88 (2016), pp. 544–557.

[22] ENTSO-E. *Task Force on Significant Frequency Deviations: External Report*. Accessed: 2024-12-03. 2019. URL: https://eepublicdownloads.entsoe.eu/clean-documents/news/2019/190522_SOC_TOP_11.6_Task%20Force%20Significant%20Frequency%20Deviations_External%20Report.pdf.

[23] Fingrid. *Maintenance of Power Balance*. https://www.fingrid.fi/en/grid/power-transmission/maintenance-of-power-balance/. Accessed: 2024-10-03. 2024.

[24] Fingrid. *Reserve Products and Reserve Market Places*. https://www.fingrid.fi/globalassets/dokumentit/en/electricity-market/reserves/reserve-products-and-reserve-market-places.pdf. Accessed: 2024-10-03. 2023.

[25] European Union. *Regulation (EU) 2019/943 of the European Parliament and of the Council*. https://eur-lex.europa.eu/legal-content/EN/TXT/PDF/?uri=CELEX:32019R0943&from=EN. Accessed: 2024-10-03. 2019.

[26] Fingrid. *Balancing Power and Capacity Markets*. https://www.fingrid.fi/en/electricity-market/reserves_and_balancing/balancing-energy-and-balancing-capacity-markets/. Accessed: 2024-10-03. 2024.

[27] Fingrid. *Imbalance Price in Finland*. https://www.fingrid.fi/globalassets/dokumentit/fi/sahkomarkkinat/tasesahko/imbalance-price-in-finland-29.8.2024.pdf. Accessed: 2024-10-03. 2024.

[28] Derek W. Bunn, John N. Inekwe, and David MacGeehan. "Analysis of the Fundamental Predictability of Prices in the British Balancing Market". In: *IEEE Transactions on Power Systems* 36.2 (2021), pp. 1309–1316. DOI: 10.1109/TPWRS.2020.3015871.

[29] William Lee Jolly. *"Hydrogen". Encyclopedia Britannica*. 2008. URL: https://www.britannica.com/science/hydrogen.

[30] P.R. Shukla et al., eds. *Climate Change 2022: Mitigation of Climate Change*. Cambridge University Press, 2022. URL: https://www.ipcc.ch/report/ar6/wg3/.

[31] Jon Durham Jeffrey Moore and Andre Eijk. *Compressors and expanders*. Ed. by Klaus Brun and Timothy Allison. 2022.

[32] Ke Liu, Chunshan Song, and Velu Subramani, eds. *Hydrogen and Syngas Production and Purification Technologies*. Wiley, 2009.

[33] Emiliana Fabbri and Thomas J. Schmidt. *Oxygen Evolution Reaction—The Enigma in Water Electrolysis*. https://doi.org/10.1021/acscatal.8b02712. 2018.

[34] Valentin Vogl, Max Åhman, and Lars J. Nilsson. "Assessment of hydrogen direct reduction for fossil-free steelmaking". In: *Journal of Cleaner Production* 203 (2018), pp. 736–745. ISSN: 0959-6526. DOI: https://doi.org/10.1016/j.jclepro.2018.08.279. URL: https://www.sciencedirect.com/science/article/pii/S0959652618326301.

[35] European Commission. *Commission Delegated Regulation (EU) 2023/1184 of 5 April 2023 supplementing Directive (EU) 2018/2001 of the European Parliament and of the Council as regards the determination of the share of renewable fuels of non-biological origin in the transport sector*. Accessed: 2023-10-02. 2023. URL: https://eur-lex.europa.eu/legal-content/EN/TXT/HTML/?uri=CELEX:32023R1184.

[36] Electricity Maps. *Electricity Consumption in Finland*. https://app.electricitymaps.com/zone/FI?lang=fi. Accessed: 2024-10-03. 2024.

[37] Luca Bertuccioli et al. "Study on development of water electrolysis in the EU". In: *Fuel cells and hydrogen joint undertaking* (2014), pp. 1–160.

[38] O. Dowson and L. Kapelevich. “SDDP.jl: a Julia package for stochastic dual dynamic programming”. In: *INFORMS Journal on Computing* 33 (1 2021), pp. 27–33. DOI: https://doi.org/10.1287/ijoc.2020.0987.

[39] SDDP.jl. *SDDP.jl Documentation*. 2024. URL: https://sddp.dev/stable/ (visited on 12/03/2024).

[40] Next Kraftwerke. *Power Trading in the Wholesale Electricity Markets: An Overview*. Accessed: 2024-10-02. 2024. URL: https://www.next-kraftwerke.be/knowledge-hub/power-trading.

[41] George Gross and David Finlay. “Generation supply bidding in perfectly competitive electricity markets”. In: *Computational & Mathematical Organization Theory* 6 (2000), pp. 83–98.

[42] Mohammad Javad Kasaei, Majid Gandomkar, and Javad Nikoukar. “Optimal management of renewable energy sources by virtual power plant”. In: *Renewable Energy* 114 (2017), pp. 1180–1188. ISSN: 0960-1481. DOI: https://doi.org/10.1016/j.renene.2017.08.010. URL: https://www.sciencedirect.com/science/article/pii/S0960148117307644.

[43] Niloofar Pourghaderi et al. “Commercial Demand Response Programs in Bidding of a Technical Virtual Power Plant”. In: *IEEE Transactions on Industrial Informatics* 14.11 (2018), pp. 5100–5111. DOI: 10.1109/TII.2018.2828039.

[44] Priyanka Shinde, Iasonas N. Kouveliotis-Lysikatos, and Mikael Amelin. “Cross-border Trading Model for a Risk-averse VPP in the Continuous Intraday Electricity Market”. In: *2022 18th International Conference on the European Energy Market (EEM)* (2022), pp. 1–6. URL: https://api.semanticscholar.org/CorpusID:253046576.

[45] Priyanka Shinde, Iasonas N. Kouveliotis-Lysikatos, and Mikael Amelin. “Multi-stage Stochastic Programming for VPP Trading in Continuous Intraday Electricity Markets”. In: *IEEE Transactions on Sustainable Energy* 13 (2021), pp. 1037–1048. URL: https://api.semanticscholar.org/CorpusID:237674661.

[46] Ioannis Boukas et al. “A deep reinforcement learning framework for continuous intraday market bidding”. In: *Machine Learning* 110 (2020), pp. 2335–2387. URL: https://api.semanticscholar.org/CorpusID:88489721.

[47] Nidhisha Mahilong et al. “Trading Strategy for Renewable Energy Sources in Day-Ahead and Continuous Intraday Market”. In: *2022 IEEE PES Innovative Smart Grid Technologies - Asia (ISGT Asia)* (2022), pp. 444–448. URL: https://api.semanticscholar.org/CorpusID:255597117.

[48] Anders Skajaa, Kristian Edlund, and Juan Miguel Morales. “Intraday Trading of Wind Energy”. In: *IEEE Transactions on Power Systems* 30 (2015), pp. 3181–3189. URL: https://api.semanticscholar.org/CorpusID:20377236.

[49] Nhung Nguyen Hong and Huy Nguyen Duc. “Virtual Power Plant’s Optimal Scheduling Strategy in Day-Ahead and Balancing Markets Considering Reserve Provision Model of Energy Storage System”. In: *Applied Sciences* (2024). URL: https://api.semanticscholar.org/CorpusID:268314327.

[50] Evaggelos G. Kardakos, Christos K. Simoglou, and Anastasios G. Bakirtzis. “Optimal Offering Strategy of a Virtual Power Plant: A Stochastic Bi-Level Approach”. In: *IEEE Transactions on Smart Grid* 7 (2016), pp. 794–806. URL: https://api.semanticscholar.org/CorpusID:25932588.

[51] Xingyu Yan et al. “An IGDT-Based Day-Ahead Co-Optimization of Energy and Reserve in a VPP Considering Multiple Uncertainties”. In: *IEEE Transactions on Industry Applications* 58 (2022), pp. 4037–4049. URL: https://api.semanticscholar.org/CorpusID:246984777.

[52] Zahid Ullah, Arshad, and Hany Hassanin. “Modeling, Optimization, and Analysis of a Virtual Power Plant Demand Response Mechanism for the Internal Electricity Market Considering the Uncertainty of Renewable Energy Sources”. In: *Energies* (2022). URL: https://api.semanticscholar.org/CorpusID:250965798.

[53] Ana R. Silva, H.M.I. Pousinho, and Ana Estanqueiro. “A multistage stochastic approach for the optimal bidding of variable renewable energy in the day-ahead, intraday and balancing markets”. In: *Energy* 258 (2022), p. 124856. ISSN: 0360-5442. DOI: https://doi.org/10.1016/j.energy.2022.124856. URL: https://www.sciencedirect.com/science/article/pii/S0360544222017595.

[54] Manuel Tobias Baumhof et al. “Optimization of Hybrid Power Plants: When is a Detailed Electrolyzer Model Necessary?” In: *2023 IEEE Belgrade PowerTech*. 2023, pp. 1–10. DOI: 10.1109/PowerTech55446.2023.10202860.

[55] Yaolong Bo et al. “Optimal Dispatch for Integrated Energy Microgrid Considering Start-up and Shutdown of Hydrogen Production”. In: *2021 IEEE 5th Conference on Energy Internet and Energy System Integration (EI2)*. 2021, pp. 2043–2047. DOI: 10.1109/EI252483.2021.9713608.

[56] Lucas Bolívar Jaramillo and Anke Weidlich. “Optimal microgrid scheduling with peak load reduction involving an electrolyzer and flexible loads”. In: *Applied Energy* 169 (2016), pp. 857–865. ISSN: 0306-2619. DOI: https://doi.org/10.1016/j.apenergy.2016.02.096. URL: https://www.sciencedirect.com/science/article/pii/S0306261916302525.

[57] Mario VF Pereira and Leontina MVG Pinto. “Multi-stage stochastic optimization applied to energy planning”. In: *Mathematical programming* 52 (1991), pp. 359–375.

[58] Anthony Papavasiliou et al. “Application of Stochastic Dual Dynamic Programming to the Real-Time Dispatch of Storage Under Renewable Supply Uncertainty”. In: *IEEE Transactions on Sustainable Energy* 9 (2018), pp. 547–558. URL: https://api.semanticscholar.org/CorpusID:4128640.

[59] Qiang Lei et al. "Optimal scheduling of a renewable energy-based park power system: A novel hybrid SDDP/MPC approach". In: *International Journal of Electrical Power Energy Systems* 157 (2024), p. 109892. ISSN: 0142-0615. DOI: https://doi.org/10.1016/j.ijepes.2024.109892. URL: https://www.sciencedirect.com/science/article/pii/S0142061524001133.

[60] Anthony Downward, Oscar Dowson, and Regan Baucke. "Stochastic dual dynamic programming with stagewise-dependent objective uncertainty". In: *Operations Research Letters* 48.1 (2020), pp. 33–39. ISSN: 0167-6377. DOI: https://doi.org/10.1016/j.orl.2019.11.002. URL: https://www.sciencedirect.com/science/article/pii/S0167637718300774.

[61] A. Downward, O. Dowson, and R. Baucke. "Stochastic dual dynamic programming with stagewise-dependent objective uncertainty". In: *Operations Research Letters* 48 (1 2020), pp. 33–39. DOI: https://doi.org/10.1016/j.orl.2019.11.002.

[62] Oscar Dowson. "Applying Stochastic Optimisation to the New Zealand Dairy Industry". PhD Thesis. PhD thesis. The University of Auckland, 2018. URL: http://hdl.handle.net/2292/37700.

[63] Priyanka Shinde and Mikael Amelin. "A Literature Review of Intraday Electricity Markets and Prices". In: *2019 IEEE Milan PowerTech*. 2019, pp. 1–6. DOI: 10.1109/PTC.2019.8810752.

[64] Dahua Lin et al. *JuliaStats/Distributions.jl: a Julia package for probability distributions and associated functions*. July 2019. DOI: 10.5281/zenodo.2647458. URL: https://doi.org/10.5281/zenodo.2647458.

[65] Gurobi Optimization, LLC. *Gurobi Optimizer Reference Manual*. 2024. URL: https://www.gurobi.com.

[66] *SKM Power System Management*. https://syspower5.skm.no. Accessed: 2024-10-03. 2024.

[67] Thomas Cokelaer. *FITTER Documentation*. Version 1.7.1, accessed November 6, 2024. 2022. URL: https://fitter.readthedocs.io/en/latest/.

[68] Wen-Chang Tsai et al. "A Review of Modern Wind Power Generation Forecasting Technologies". In: *Sustainability* 15.14 (2023). URL: https://www.mdpi.com/2071-1050/15/14/10757.

[69] H. Miinusmaa. "Nelikulmaisen reiän poraamisesta kolmikulmaisella poralla". Diplomityö. Espoo: Teknillinen korkeakoulu, konetekniikan osasto, 1977.

[70] ENTSO-E. *Generation Forecasts - Day Ahead for Wind and Solar*. Accessed: 2024-11-06. 2024. URL: https://transparency.entsoe.eu/content/static_content/Static%20content/knowledge%20base/data-views/generation/Data-view%20Generation%20Forecasts%20-%20Day%20Ahead%20for%20Wind%20and%20Solar.html.

[71] Sergei Kulakov and Florian Ziel. “The Impact of Renewable Energy Forecasts on Intraday Electricity Prices”. In: *Economics of Energy & Environmental Policy* (2019). URL: https://api.semanticscholar.org/CorpusID:85498758.

[72] Nord Pool Group. *Transition to 15-minute Market Time Unit (MTU)*. https://www.nordpoolgroup.com/en/trading/transition-to-15-minute-market-time-unit-mtu/. Accessed: 2024-11-11.